Optimal control methods for quantum batteries

Francesco Mazzoncini,[1,2,*] Vasco Cavina,[2,3] Gian Marcello Andolina,[2,4]
Paolo Andrea Erdman,[5] and Vittorio Giovannetti[2]

[1]*Télécom Paris–LTCI, Institut Polytechnique de Paris, 19 Place Marguerite Perey, 91120 Palaiseau, France*
[2]*NEST, Scuola Normale Superiore, I-56126 Pisa, Italy*
[3]*Department of Physics and Materials Science, University of Luxembourg, L-1511 Luxembourg, Luxembourg*
[4]*Institut de Ciències Fotòniques, The Barcelona Institute of Science and Technology, Avenida Carl Friedrich Gauss 3, 08860 Castelldefels (Barcelona), Spain*
[5]*Department of Mathematics and Computer Science, Freie Universität Berlin, Arnimallee 6, 14195 Berlin, Germany*

(Received 8 November 2022; accepted 2 March 2023; published 30 March 2023)

We investigate the optimal charging processes for several models of quantum batteries, finding how to maximize the energy stored in a given battery with a finite-time modulation of a set of external fields. We approach the problem using advanced tools of optimal control theory, highlighting the universality of some features of the optimal solutions, for instance the emergence of the well-known bang-bang behavior of time-dependent external fields. The technique presented here is general, and we apply it to specific cases in which the energy is either pumped into the battery by external forces (direct charging) or transferred into it from an external charger (mediated charging). In this paper we focus on particular systems that consist of coupled qubits and harmonic oscillators, for which the optimal charging problem can be explicitly solved using a combined analytical-numerical approach based on our optimal control techniques. However, our approach can be applied to more complex setups, thus fostering the study of many-body effects in the charging process.

DOI: 10.1103/PhysRevA.107.032218

I. INTRODUCTION

In recent years, with the rapid development of new quantum technologies [1,2], there has been a worldwide interest in exploiting quantum phenomena that arise at a microscopic level. Here, we will focus on studying the so-called quantum batteries [3–10], i.e., quantum-mechanical systems employed for energy storage, where quantum effects can be used to obtain more efficient and faster charging processes than classical systems.

This blossoming research field has to address many different questions, such as the stabilization of stored energy [11,12], the practical implementation of quantum batteries [13,14], and the study of optimal charging processes [7,8,15], offering a vast research panorama on both theoretical [11–13,16–24] and experimental ends [14,25]. Within this framework, we will derive optimal charging strategies for quantum batteries using techniques from quantum control theory [26–30], a powerful mathematical tool that has many applications in different fields of physics such as quantum optics [31,32] and physical chemistry [33–35]. Quantum control theory has contributed to understanding interesting aspects of quantum mechanics such as the quantum speed limit [36–39] and to generate efficient quantum gates in open quantum systems [40,41]. In this paper, we study how a qubit or a quantum harmonic oscillator can be optimally charged with a modulation of an external Hamiltonian. In order to find the best charging protocol we will use Pontryagin's minimum principle (PMP) [42,43], a very useful theorem of classical optimal control theory, which is frequently used also in quantum control theory [44–48]. We show that, in most cases that we consider, quantum batteries can be optimally charged through different variants of a so-called bang-bang modulation of the intensity of an external Hamiltonian.

Our paper is organized as follows. In Sec. II we introduce two general charging protocols to inject energy in a quantum battery. In Sec. III we present a brief introduction to Pontryagin's minimum principle, highlighting the main tools that we shall use throughout the paper. In Sec. IV we focus on the first charging protocol, consisting of a closed system charged by the modulation of an external Hamiltonian. Section V provides a more detailed analysis of the charging of specific examples, such as the single qubit or the harmonic oscillator. Section VI is devoted to analyzing a second charging process, where we make use of the coupling between a quantum battery and an auxiliary quantum system. Finally, a brief summary of our main conclusions is reported in Sec. VII, while useful technical details can be found in the Appendices.

II. CHARGING OF A QUANTUM BATTERY

We start by defining two general protocols for the charging process of a quantum battery (see Fig. 1 for a pictorial representation).

A. Direct charging process

The first charging model consists of a single closed quantum system initialized in a state $\rho(0)$ that evolves in time

*mazzoncini@telecom-paris.fr

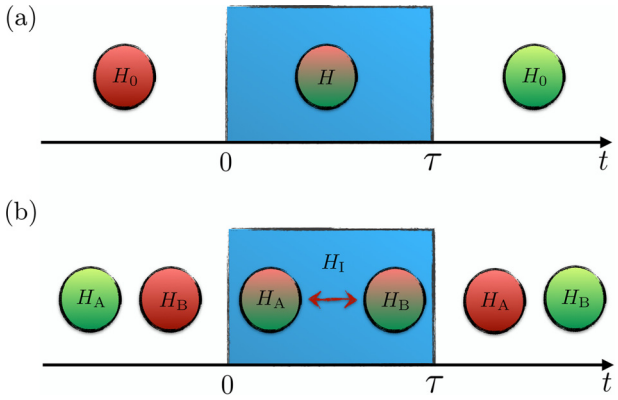

FIG. 1. (a) Direct charging process: charging model for a closed system through the modulation of an external control for a finite amount of time τ. (b) Mediated charging process: it consists in letting two systems A and B interact through a Hamiltonian H_1.

under the action of a time-dependent Hamiltonian of the form

$$H(t) = H_0 + \boldsymbol{\lambda}(t)\cdot\mathbf{H} := H_0 + \sum_{i=1}^{m}\lambda_i(t)H_i. \tag{1}$$

In this expression H_0 is the *intrinsic* Hamiltonian contribution which defines the energy content of the system before and after the charging process and $\mathbf{H} := (H_1, \ldots, H_m)$ is a collection of *charging* Hamiltonian terms which are modulated by control functions $\boldsymbol{\lambda}(t) := (\lambda_1(t), \ldots, \lambda_m(t))$ that we assume to be active (i.e., different from zero) only over a limited time interval $[0, \tau]$. They can take values that are determined by some assigned constraint, i.e., $\boldsymbol{\lambda}(t) \in \mathbb{D}[0, \tau]$, where $\tau > 0$ is the total duration of the charging process and $\mathbb{D}[0, \tau]$ is a proper subset of the real functions $\mathbb{F}[0, \tau]$ mapping $[0, \tau]$ into $\mathbb{R}^m$. Our goal is hence to find an optimal $\boldsymbol{\lambda}^\star(t) \in \mathbb{D}[0, \tau]$ that, given an assigned τ, maximizes the mean energy of the system at the end of the process. Introducing

$$U_\tau := \mathcal{T}\exp\left[-i\int_0^\tau dt\, H(t)\right], \tag{2}$$

the time-ordered unitary evolution operator associated with the time-dependent Hamiltonian (1), and

$$\rho(\tau) = U_\tau\rho(0)U_\tau^\dagger, \tag{3}$$

the evolved state of the system at time τ, we aim to determine the quantity

$$E_{\max}(\tau) := E(\tau)|_{\boldsymbol{\lambda}^\star(t)} = \max_{\boldsymbol{\lambda}(t)\in\mathbb{D}[0,\tau]} E(\tau), \tag{4}$$

where using $\langle\cdot\rangle$ as a short-hand notation to indicate the trace operator we set

$$E(\tau) := \langle\rho(\tau)H_0\rangle \tag{5}$$

(notice that hereafter we have set $\hbar = 1$). It is worth pointing out that since the direct charging process (DCP) models considered here rely on closed dynamical evolutions (no interactions with external degrees of freedom being allowed) the DCP optimization we are targeting corresponds also to maximizing the amount of *extractable work* we can store in the system as measured by the ergotropy, the total ergotropy, or the thermal free energy [49]. To see this explicitly we recall that given a quantum system with Hamiltonian $H(t)$ and state $\rho(t)$ all these quantities can be computed as

$$\mathcal{W}[\rho(t), H(t)] := \langle\rho(t)H(t)\rangle - \mathcal{F}(s_{\rho(t)}, s_{H(t)}), \tag{6}$$

where $\mathcal{F}(s_{\rho(t)}, s_{H(t)})$ is a functional that only depends upon the collections $s_{\rho(t)} = \{\eta_1(t), \eta_2(t), \ldots\}$ and $s_{H(t)} = \{\epsilon_1(t), \epsilon_2(t), \ldots\}$ of the eigenvalues of ρ and H, respectively (see Appendix A for details). Since the unitary evolution (3) preserves $s_{\rho(t)}$, and $s_{H(\tau)} = s_{H_0}$ in the DCP, $\mathcal{F}(s_{\rho(\tau)}, s_{H(\tau)}) = \mathcal{F}(s_{\rho(0)}, s_{H_0})$ so that this quantity plays no role in the optimization procedure.

B. Mediated charging process

Although the DCP is of undoubted theoretical interest, a closed evolution of a unique system is not genuinely realistic from the physical implementation point of view. Such a unitary evolution regime occurs only when the dynamics of the energy source are very slow compared to the quantum battery dynamics (i.e., in the Born-Oppenheimer limit). Therefore, we also consider a second charging model, called the mediated charging process (MCP) [4,5], that involves instead two separate elements: an auxiliary quantum system A, called the charger, and a quantum battery B. In the MCP we aim at maximizing the energy stored in B by suitably modulating its interaction with A in finite time τ. For this reason we replace the DCP Hamiltonian (1) with

$$H(t) := H_A + H_B + \boldsymbol{\lambda}(t)\cdot\mathbf{H}, \tag{7}$$

where H_A and H_B are local operators of A and B, respectively, and $\boldsymbol{H}$ is now free to act on both the battery and the auxiliary system. The quantity to optimize is now given by

$$E_B(\tau) := \langle\rho_B(\tau)H_B\rangle, \tag{8}$$

where $\rho_B(\tau)$ is the reduced density matrix of the battery at time τ. Since $\rho_B(\tau)$ does not follow a unitary trajectory in the MCP scenario, $s_{\rho_B(\tau)}$ is typically different from $s_{\rho_B(0)}$, which implies that $\mathcal{W}[\rho_B(\tau), H_B]$ is considerably more challenging to optimize. We shall see however that by choosing wisely the global initial state $\rho_{AB}(0)$ we can reduce our analysis to simpler DCPs, as shown in Sec. VI.

III. PONTRYAGIN'S MINIMUM PRINCIPLE

PMP [43] is the main tool we will use in the optimization of DCPs and MCPs and will allow us to formally identify necessary conditions for the optimality of $\boldsymbol{\lambda}^\star(t)$. Here we introduce the approach to optimal control problems provided by PMP using a general formalism, that will be adapted to both DCP and MCP problems afterwards. Consider a set of *state variables* at a given time t, represented by the elements of a vector $\boldsymbol{v}(t) := (v_1(t), \ldots, v_n(t))$ which evolves via a dynamical equation represented by n first-order differential equations of the form

$$\dot{\boldsymbol{v}}(t) = \boldsymbol{f}(\boldsymbol{v}(t), \boldsymbol{\lambda}(t), t), \tag{9}$$

with $\boldsymbol{f}$ a vectorial function. The quantity to optimize, also called the *performance criterion*, is evaluated in terms of a

cost function written as

$$J = \int_0^\tau g(\boldsymbol{v}(t), \boldsymbol{\lambda}(t), t)dt, \tag{10}$$

with g a scalar function. Defining the *pseudo-Hamiltonian* $\mathcal{H}$ as

$$\mathcal{H} := g(\boldsymbol{v}(t), \boldsymbol{\lambda}(t), t) + \boldsymbol{p}(t) \cdot \boldsymbol{f}(\boldsymbol{v}(t), \boldsymbol{\lambda}(t), t), \tag{11}$$

with $\boldsymbol{p}(t)$ the n-dimensional row vector of Lagrange multipliers, called *costates*, the PMP states that necessary conditions for an optimal control $\boldsymbol{\lambda}^\star(t) \in \mathbb{D}[0, \tau]$ to minimize J are that for all $t \in [0, \tau]$:

$$\begin{aligned}
&\dot{\boldsymbol{v}}(t) = \frac{\partial \mathcal{H}}{\partial \boldsymbol{p}}(\boldsymbol{v}(t), \boldsymbol{\lambda}^\star(t), \boldsymbol{p}(t), t),\\
&\dot{\boldsymbol{p}}(t) = -\frac{\partial \mathcal{H}}{\partial \boldsymbol{v}}(\boldsymbol{v}(t), \boldsymbol{\lambda}^\star(t), \boldsymbol{p}(t), t),\\
&\mathcal{H}(\boldsymbol{v}(t), \boldsymbol{\lambda}^\star(t), \boldsymbol{p}(t), t) \leqslant \mathcal{H}(\boldsymbol{v}(t), \boldsymbol{\lambda}(t), \boldsymbol{p}(t), t),\\
&\qquad\qquad\qquad\qquad\qquad\qquad \forall \boldsymbol{\lambda}(t) \in \mathbb{D}[0, \tau].
\end{aligned} \tag{12}$$

Moreover, the PMP gives additional constraints based on the boundary conditions of our problem, i.e., whether the final state and the final time are fixed or free. In particular, (1) if the final time τ is fixed and no constraint is posed on the final state $\boldsymbol{v}(\tau)$, then

$$\boldsymbol{p}(\tau) = (0, 0, \cdots, 0); \tag{13}$$

(2) if the final time τ is free while the final state $\boldsymbol{v}(\tau)$ is fixed, then

$$\mathcal{H}(\boldsymbol{v}(\tau), \boldsymbol{\lambda}^\star(\tau), \boldsymbol{p}(\tau), \tau) = 0. \tag{14}$$

We finally highlight that the PMP is not the only possible optimization method to analyze charging processes for quantum batteries. For instance, Ref. [15] deploys an iterative approach to minimize the distance between the target state and the final state, considering a variant of our charger-mediated process where a modulated field is acting only on the charger, considered in this case as an open dissipative system. However, since PMP gives necessary conditions for optimality, any other optimization method must eventually satisfy those conditions.

IV. DCP OPTIMAL SOLUTIONS

In this section we will derive the optimal solutions for DCPs considering two different settings: first in Sec. IV A we fix the total duration of the charging event τ and try to identify the optimal pulse $\boldsymbol{\lambda}^\star(t)$ which, starting from a given initial configuration $\rho(0)$, produces the maximum value of the output energy $E_{\max}(\tau)$; then in Sec. IV B we analyze the dual problem, that is, we fix a target output state that ensures a certain value of the final energy and try to find the optimal control $\boldsymbol{\lambda}^\star(t)$ that enables us to reach it in the minimum time τ.

A. Maximum output energy at fixed time τ

To begin with, we observe that if (i) the charging Hamiltonian terms H_i's are generators of the group $\mathcal{U}$ of the unitary operators on the system and (ii) no restrictions are imposed on the choice of the control vector $\boldsymbol{\lambda}(t)$, allowing $\mathbb{D}[0, \tau]$ to include all possible elements $\mathbb{F}[0, \tau]$, then the dynamical evolutions (2) can span the entire set $\mathcal{U}$ of unitary transformations on the system. Accordingly under conditions (i) and (ii) we can write

$$\begin{aligned}
E_{\max}(\tau) &= \max_{\boldsymbol{\lambda}(t) \in \mathbb{F}[0,\tau]} \langle U_\tau \rho(0) U_\tau^\dagger H_0 \rangle\\
&= \max_{U \in \mathcal{U}} \langle U \rho(0) U^\dagger H_0 \rangle =: \overline{E}_{\max},
\end{aligned} \tag{15}$$

where $\overline{E}_{\max}$ is a τ independent constant that represents the maximum amount of energy we can force into the system via arbitrary unitary manipulations. The constant $\overline{E}_{\max}$ can be explicitly evaluated as

$$\overline{E}_{\max} = \sum_{i=1} \eta_i^\uparrow(0)\, \epsilon_i^\uparrow(0), \tag{16}$$

with $s^\uparrow_{\rho(0)} = \{\eta_1^\uparrow(0), \eta_2^\uparrow(0), \dots\}$ and $s^\uparrow_{H_0} = \{\epsilon_1^\uparrow(0), \epsilon_2^\uparrow(0), \dots\}$ being the spectra of $\rho(0)$ and H_0, rearranged in increasing order. Note that it is possible to establish a direct connection between $\overline{E}_{\max}$ and the antiergotropy [50] of the system (see Appendix A for details). Apart from this special case, the explicit evaluation of $E_{\max}(\tau)$ is typically rather demanding and does not admit a closed analytical solution. One possible approach to tackle it is to make use of optimal control techniques. In particular, in what follows we shall rely on the PMP we have reviewed in Sec. III. For this purpose we rewrite the final energy (5) as

$$E(\tau) = \int_0^\tau \langle H_0 \dot{\rho}(t) \rangle dt + E(0), \tag{17}$$

where $\dot{\rho}(t) = \mathcal{N}[\rho(t)] = -i[H(t), \rho(t)]$. Accordingly, we can study the optimization of the charging process as a minimization problem of the cost function:

$$J := -\int_0^\tau \langle H_0 \mathcal{N}[\rho(t)] \rangle dt. \tag{18}$$

The optimization task can then be translated into a PMP problem by introducing the following arrangements:

$$\begin{aligned}
&\boldsymbol{v}(t) \to \rho(t), \quad \boldsymbol{\lambda}(t) \to \boldsymbol{\lambda}(t), \quad \boldsymbol{p}(t) \to \pi(t),\\
&\boldsymbol{f}(\boldsymbol{v}(t), \boldsymbol{\lambda}(t), t) \to \mathcal{N}[\rho(t)],\\
&g(\boldsymbol{v}(t), \boldsymbol{\lambda}(t), t) \to -\langle H_0 \mathcal{N}[\rho(t)] \rangle,\\
&\boldsymbol{p}(t) \cdot \boldsymbol{f}(\boldsymbol{x}(t), \boldsymbol{\lambda}(t), t) \to \langle \pi(t) \mathcal{N}[\rho(t)] \rangle,
\end{aligned} \tag{19}$$

with $\pi(t)$ being a self-adjoint operator of the same dimension of $\rho(t)$, and defining the pseudo-Hamiltonian

$$\begin{aligned}
\mathcal{H}(\rho(t), \boldsymbol{\lambda}(t), \pi(t), t) &:= \langle [\pi(t) - H_0] \mathcal{N}[\rho(t)] \rangle\\
&= \boldsymbol{\lambda}(t) \cdot \boldsymbol{G}(t) - i \langle \pi'(t) [H_0, \rho(t)] \rangle,
\end{aligned} \tag{20}$$

with $\pi'(t) := \pi(t) - H_0$ and $\boldsymbol{G}(t) := (G_1(t), \dots, G_m(t))$ being a column vector of elements:

$$G_j(t) := -i \langle \pi'(t) [H_j, \rho(t)] \rangle. \tag{21}$$

This allows us to express the necessary conditions (12) for the optimal control vector $\boldsymbol{\lambda}^\star(t)$ as

$$\begin{aligned}
&\dot{\rho}(t) = -i\big[H^\star(t), \rho(t)\big],\\
&\dot{\pi}'(t) = -i[H^\star(t), \pi'(t)],\\
&\boldsymbol{\lambda}^\star(t)\cdot\boldsymbol{G}(t) \leqslant \boldsymbol{\lambda}(t)\cdot\boldsymbol{G}(t), \quad \forall\boldsymbol{\lambda}(t)\in\mathbb{D}[0,\tau],
\end{aligned} \tag{22}$$

where $H^\star(t)$ represents the Hamiltonian (1) evaluated on the optimal control pulse, i.e.,

$$H^\star(t) := H_0 + \boldsymbol{\lambda}^\star(t)\cdot\mathbf{H}. \tag{23}$$

In the third line of Eq. (22) we exploited Eq. (20) and the fact that the term $-i\langle\pi'(t)[H_0,\rho(t)]\rangle$ does not depend explicitly on $\boldsymbol{\lambda}(t)$. In the case of a charging process with fixed time τ and unknown optimal final state $\rho(\tau)$, the list (22) has to be completed with the extra condition (13) which in the present case becomes

$$\pi(\tau) = 0 \quad\Longleftrightarrow\quad \pi'(\tau) = -H_0. \tag{24}$$

The first two equations in (22) simply tell us that $\rho(t)$ and $\pi'(t)$ represent the state and the costate operator of the system evolved under the action of the Hamiltonian (23). What ultimately decides whether a given $\boldsymbol{\lambda}^\star(t)$ has a chance of being an optimal solution is the inequality in Eq. (22) which, unfortunately, due to the implicit dependence upon $\boldsymbol{\lambda}^\star(t)$ of $\boldsymbol{G}(t)$, is typically not analytically treatable. Nonetheless, in the special special case where we have a unique control function (i.e., $m = 1$) and the allowed domain $\mathbb{D}[0,\tau]$ is chosen to simply force the intensity of $\lambda_1(t)$ to belong to a given interval $\mathcal{I}_1 = [\lambda_1^{\min}, \lambda_2^{\max}]$, the inequality in Eq. (22) translates into a series of (simplified) conditions which provide us with a nice guidance on how to construct the optimal control pulse.

(a) $\lambda_1^\star(t)$ can take the *minimum* allowed value $\lambda_1^{\min}$ if and only if the associated $G_1(t)$ function is strictly positive, i.e.,

$$\lambda_1^\star(t) = \lambda_1^{\min} \quad\Longleftrightarrow\quad G_1(t) > 0.$$

(b) $\lambda_1^\star(t)$ can take the *maximum* allowed value $\lambda_1^{\max}$ if and only if the associated $G_1(t)$ function is strictly negative, i.e.,

$$\lambda_1^\star(t) = \lambda_1^{\max} \quad\Longleftrightarrow\quad G_1(t) < 0.$$

(c) $\lambda_1^\star(t)$ can take arbitrary values in the allowed domain $\mathcal{I}_1 := [\lambda_1^{\min}, \lambda_1^{\max}]$ if and only if the associated $G_1(t)$ is equal to zero.

From the above analysis it emerges that natural candidates for $\lambda_1^\star(t)$ are *bang-bang*-like step functions similar to the one shown in Fig. 2 which alternate their values among the allowed extreme $\lambda_1^{\min}$ and $\lambda_1^{\max}$ with switching points corresponding to the zeros of the associated function $G_1(t)$. The only allowed exception to this rule is when $G_1(t)$ is zero over an extended interval (*singular interval* scenario): in this case the necessary conditions in Eq. (22) give no information about how to select $\lambda_1^\star(t)$ without specifying the nature of the system. Interestingly enough, a meticulous analysis of singular intervals has already turned out to be crucial in analyzing optimal-time controls for dissipative quantum systems [51,52].

B. Minimum charging time at fixed final state

Another problem that we can tackle using the PMP method is to determine the minimum value of the charging time τ that allows us to move our initial state $\rho(0)$ into a final target configuration $\rho_\diamond$—for instance a state in which the eigenvalues are sorted in increasing order which according to Eq. (16) grants us the maximum value of the stored final energy $\overline{E}_{\max}$ allowed by the most general DCP process. The new cost function of the problem can be written as

$$J := -\int_0^\tau 1dt, \tag{25}$$

which is a simple way to express the charging time in an integral form. With the same notations adopted in the previous section, we can hence define the pseudo-Hamiltonian of the new problem as

$$\begin{aligned}
\mathcal{H}(\rho(t),\boldsymbol{\lambda}(t),\pi(t),t) &:= \langle\pi(t)\mathcal{N}[\rho(t)]\rangle - 1\\
&= \boldsymbol{\lambda}(t)\cdot\boldsymbol{G}(t) - i\langle\pi(t)[H_0,\rho(t)]\rangle - 1,
\end{aligned}$$

where now $\boldsymbol{G}(t)$ is the vector of components:

$$G_j(t) = -i\langle\pi(t)[H_j,\rho(t)]\rangle. \tag{26}$$

Doing almost the same calculations that led us to Eq. (22), we can hence cast the PMP constraint (12) for the optimal pulse $\boldsymbol{\lambda}^\star(t)$ that leads to the target state $\rho_\diamond$ in the minimal time τ, in the following form:

$$\begin{aligned}
&\dot{\rho}(t) = -i[H^\star(t),\rho(t)],\\
&\dot{\pi}(t) = -i[H^\star(t),\pi(t)],\\
&\boldsymbol{\lambda}^\star(t)\cdot\boldsymbol{G}(t) \leqslant \boldsymbol{\lambda}(t)\cdot\boldsymbol{G}(t), \quad \forall\boldsymbol{\lambda}(t)\in\mathbb{D}[0,\tau],
\end{aligned} \tag{27}$$

where $H^\star(t)$ is again defined as in (23), with the new extra condition imposed by (14),

$$\langle\pi(\tau)[H^\star(\tau),\rho_\diamond]\rangle = i, \tag{28}$$

replacing Eq. (24). Notice that also in this case $\rho(t)$ and the costate $\pi(t)$ undergo the same temporal dynamics; however, in the present problem the final value of the costate is only partially determined by the new constraint Eq. (28). We also point out that as for (22) simplifications arise when there is

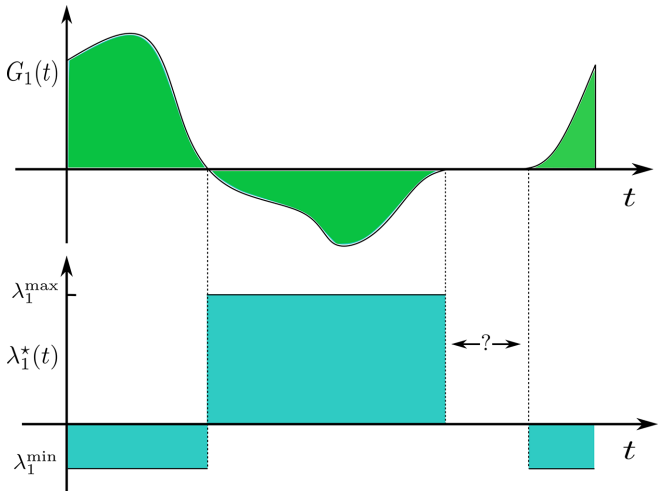

FIG. 2. Example of the relationship between a time-optimal control $\lambda_1^\star(t)$ and the switching function $G_1(t)$ for the case in which the system is characterized by a single control function ($m = 1$). The region with a question mark is a singular interval, where the value of the optimal control is not determined by the conditions in Eq. (22).

only one control parameter $m = 1$ with constrained intensity $\lambda_1(t) \in \mathcal{I}_1$, which allows one to translate the third equation of (27) into the same (a), (b), and (c) rules detailed in the previous section.

V. EXAMPLES OF DCP MODELS

Here we analyze in detail some examples of DCP models: a qubit with one ($m = 1$) or two ($m = 2$) charging fields, and a harmonic oscillator under the action of a linear time-dependent perturbation.

A. Qubit optimal DCP with a single charging field

In this section we focus on a first example of DCP where the system of interest is represented by a single qubit which is controlled via a single control field (i.e., $m = 1$). For the Hamiltonian (1) we select

$$H_0 = \frac{\omega_0}{2}(\mathbb{1} - \sigma_z), \qquad H_1 = \boldsymbol{x}\cdot\boldsymbol{\sigma}, \tag{29}$$

with $\boldsymbol{x} := (x_1, x_2, x_3)$ a unit row vector of real components and $\boldsymbol{\sigma} := (\sigma_x, \sigma_y, \sigma_z)^T$ the Pauli column vector.

Let us start by observing that whenever $\boldsymbol{x}$ is not pointing the z direction H_1 and H_0 form a generator set for the $su(2)$ algebra. Accordingly, despite the limited number of charging terms, if no restrictions are posed on the intensity of the control function $\lambda_1(t)$ or, alternatively, if the charging time τ is sufficiently large, the transformations (2) we can induce on the system are still capable of spanning the entire unitary space $\mathcal{U}$ and one recovers the result (15), i.e.,

$$E_{\max}(\tau)|_{\text{unbounded}} = \overline{E}_{\max} = \omega_0\left(\frac{1 + |\boldsymbol{a}(0)|}{2}\right), \tag{30}$$

where, given $\boldsymbol{a}(0)$ as the Bloch vector of the initial state $\rho(0)$, $[1 + |\boldsymbol{a}(0)|]/2$ is the maximum eigenvalue of such a state. To study the case where instead $\lambda_1(t)$ is forced to belong to a finite interval $\mathcal{I}_1 = [\lambda_1^{\min}, \lambda_1^{\max}]$, we use the PMP method detailed at the end of the previous section. In this particular case, $\pi'(\tau)$ is a 2×2 Hermitian matrix with trace $-\omega_0$. Since the unitary evolution preserves the trace, we can always write the state and the costate as

$$\begin{aligned}\rho(t) &= \frac{\mathbb{1} + \boldsymbol{a}(t)\cdot\boldsymbol{\sigma}}{2},\\ \pi'(t) &= -\omega_0\frac{\mathbb{1} + \boldsymbol{b}(t)\cdot\boldsymbol{\sigma}}{2},\end{aligned} \tag{31}$$

where $\boldsymbol{a}(t)$ and $\boldsymbol{b}(t)$ are two unit row vectors with $\boldsymbol{a}(0)$ being the Bloch vector of the input state of the system and $\boldsymbol{b}(\tau) = (0, 0, -1)$. Replacing this into (5) and Eq. (21) we hence get $E(\tau) = (\omega_0/2)\,[1 - a_3(\tau)]$, where $a_3(\tau)$ is the z component of $\boldsymbol{a}(\tau)$, and

$$\begin{aligned}G_1(t) &= -\,i\langle\pi'(t)[H_1, \rho(t)]\rangle = \frac{i\omega_0}{4}\langle\boldsymbol{b}(t)\cdot\boldsymbol{\sigma}[\boldsymbol{x}\cdot\boldsymbol{\sigma}, \boldsymbol{a}(t)\cdot\boldsymbol{\sigma}]\rangle\\ &= -\,\omega_0\,\boldsymbol{b}(t)\cdot\boldsymbol{x}\wedge\boldsymbol{a}(t) = \omega_0\,\boldsymbol{x}\cdot\boldsymbol{b}(t)\wedge\boldsymbol{a}(t).\end{aligned} \tag{32}$$

The crucial case $G_1(t) = 0$ can then be translated into the condition

$$G_1(t) = 0 \iff \boldsymbol{x}\cdot\boldsymbol{b}(t)\wedge\boldsymbol{a}(t) = 0. \tag{33}$$

As discussed in Appendix B this corresponds to the identity

$$\lambda_1^\star(t) = \frac{\omega_0}{2}x_3 \tag{34}$$

as the constraint that leads to a singular interval, with x_3 the third component of the unit vector $\boldsymbol{x}$. Following the indications of the PMP detailed in the previous section, we can hence claim that for the DCP model we are considering here the optimal choice for the control parameter $\lambda_1^\star(t)$ must be indeed a bang-bang protocol represented by a piecewise-constant function that on the interval $[0, \tau]$ takes values extracted from the three-element set $\mathcal{S} = \{\lambda_1^{\min}, \frac{\omega_0}{2}x_3, \lambda_1^{\max}\}$ for $\frac{\omega_0}{2}x_3 \in \mathcal{I}_1$, or from the two-element set $\mathcal{S} = \{\lambda_1^{\min}, \lambda_1^{\max}\}$ if $\frac{\omega_0}{2}x_3 \notin \mathcal{I}_1$. Specifically, given a $(N+1)$-elements partition $\mathcal{P}$ of the charging interval $[0, \tau]$,

$$0 = t_0 < t_1 < \cdots < t_N < t_{N+1} = \tau, \tag{35}$$

and a collection $\mathcal{L} := \{\Lambda_1, \Lambda_2, \ldots, \Lambda_{N+1}\}$ of elements extracted from the set $\mathcal{S}$, we can write

$$\lambda_1^\star(t) = \sum_{k=1}^{N+1}\Lambda_k\ \text{Step}_{\Delta t_k}[t - t_{k-1}], \tag{36}$$

where for all $k = \{1, \ldots, N+1\}$ we have $\Delta t_k := t_k - t_{k-1}$, and where

$$\text{Step}_{\Delta T}[t] := \begin{cases}1 & \forall t \in [0,\ \Delta T[,\\ 0 & \text{otherwise}\end{cases} \tag{37}$$

is a step function of length ΔT. This is clearly a huge simplification of the optimization problem which highlights the strength of the PMP approach. Unfortunately the identification of the specific values of N, $\mathcal{P}$, and $\mathcal{L}$ goes beyond the possibility offered by this method and they need to be addressed case by case. To confirm our theoretical reasoning we performed a numerical simulation for the special case in which at time $t = 0$ the battery is in its ground state, i.e., $\rho(0) = |0\rangle\langle 0|$ or equivalently $\boldsymbol{a}(0) = (0, 0, 1)$. Furthermore, to simplify the numerical simulation, we consider the charging Hamiltonian in Eq. (29) to be $H_1 = \sigma_x$ selecting $\boldsymbol{x} = (1, 0, 0)$, and we fix $\lambda_1^{\min} = 0$ so that the set of allowed pulses $\mathcal{S}$ reduces to $\{0, \lambda_1^{\max}\}$. With these choices all the candidates for $\lambda^\star(t)$ are given by simple bang-bang pulses with alternating values of $\lambda_1^{\max}$ and zero (see Fig. 3). Excluding the sequences which have $\lambda_1 = 0$ in the first interval that are clearly suboptimal (with such a choice nothing is going to happen to the system at least until $t = t_2$), a complete parametrization of the PMP candidates (36) can hence be obtained in terms of the time intervals of the selected partition $\mathcal{P}$, i.e., $\Delta t_1, \Delta t_2, \ldots, \Delta t_{N+1}$, such that $\sum_{i=1}^{N+1}\Delta t_i = \tau$. Choosing different sequences of the $\Delta t_k'$s will generate different trajectories and different values of the final energy $E(\tau) = E(\Delta t_1,\ \Delta t_2, \ldots,\ \Delta t_{N+1})$ which can be explicitly computed case by case.

Setting $\lambda_1^{\max} = 0.3\omega_0$, we have run a numerical simulation of the problem for different values of the total charging

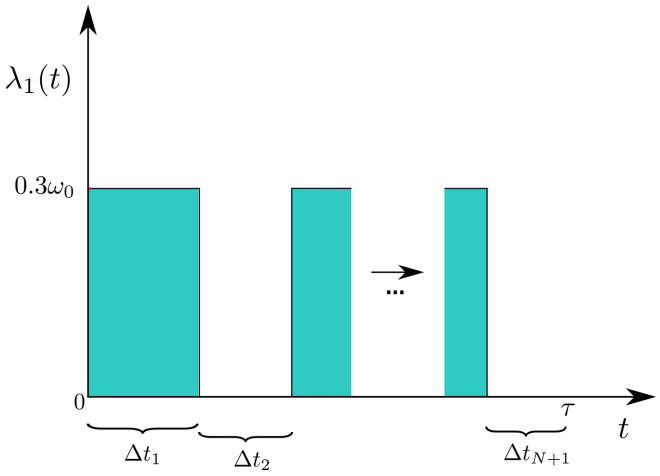

FIG. 3. Example of an optimal control PMP candidate (36) with N switches for the single-qubit DCP problem with $\boldsymbol{x} = (1, 0, 0)$ and $\lambda_1^{\min} = 0$: it corresponds to a bang-bang function that oscillates between zero and $\lambda_1^{\max}$ at the switching times t_k of the selected partition (35).

time τ selected in the domain $[0, 15/\omega_0]$, with different sets of time intervals $\Delta t_j'$s. The obtained results are summarized in Fig. 4, which reports the maximum $E_{\max}^{\text{num}}(\tau)$ of the final energy $E(\Delta t_1, \Delta t_2, \ldots, \Delta t_{N+1})$ we have obtained by running a numerical search on bang-bang functions of the type Fig. 3 organized in groups of increasing values of N. Specifically, the blue curve reports results obtained for $N \leqslant 1$ (i.e., piecewise-constant functions with up to two intervals $\Delta t_j'$s), the dotted green curve reports those for $N \leqslant 3$, and the red curve reports those for $N \leqslant 5$. The first thing that one can notice is that, as predicted in Eq. (30), for τ sufficiently large (specifically for $\tau \gtrsim 14.0\omega_0$), $E_{\max}^{\text{num}}(\tau)$ reaches the value of ω_0, which for the selected choice of the input state corresponds to the absolute maximum $\overline{E}_{\max}$. The plot shows also that in order to achieve these results we had to use piecewise-constant functions with $N = 5$. In contrast, having $N = 1$ or 3 is just enough to push $E_{\max}^{\text{num}}(\tau)$ up to $\approx 0.26\overline{E}_{\max}$ and $\approx 0.78\overline{E}_{\max}$ (dash-dotted blue and dotted green plateaus in Fig. 4). Another element which emerges from the above discussion is that, even though $E_{\max}^{\text{num}}(\tau)$ is explicitly nondecreasing in τ, it exhibits a staircaselike behavior with extended plateau regions. This means that increasing the final time does not necessarily lead to an increment of the final energy. On the contrary, by allowing for negative values of the intensity of the control, one can drastically increase the performance, getting rid of the plateaus and obtaining a monotonically increasing function for $E_{\max}^{\text{num}}(\tau)$ (this will be extensively discussed in Sec. V B). Naturally, since the analysis relies on a numerical optimization performed on a selected class of bang-bang functions with a limited (up to $N + 1 = 6$) number of switching times, one cannot exclude that enlarging the pool of candidates (e.g., increasing N) would also remove the staircase behavior; however, we believe that this is a typical feature of the constraint on the intensity of the control we have chosen, an interpretation that is validated by the fact that $E_{\max}^{\text{num}}(\tau)$ is not staircaselike if we allow $\lambda_1(t)$ to be negative. Our final remark concerns the consistency of the obtained numerical

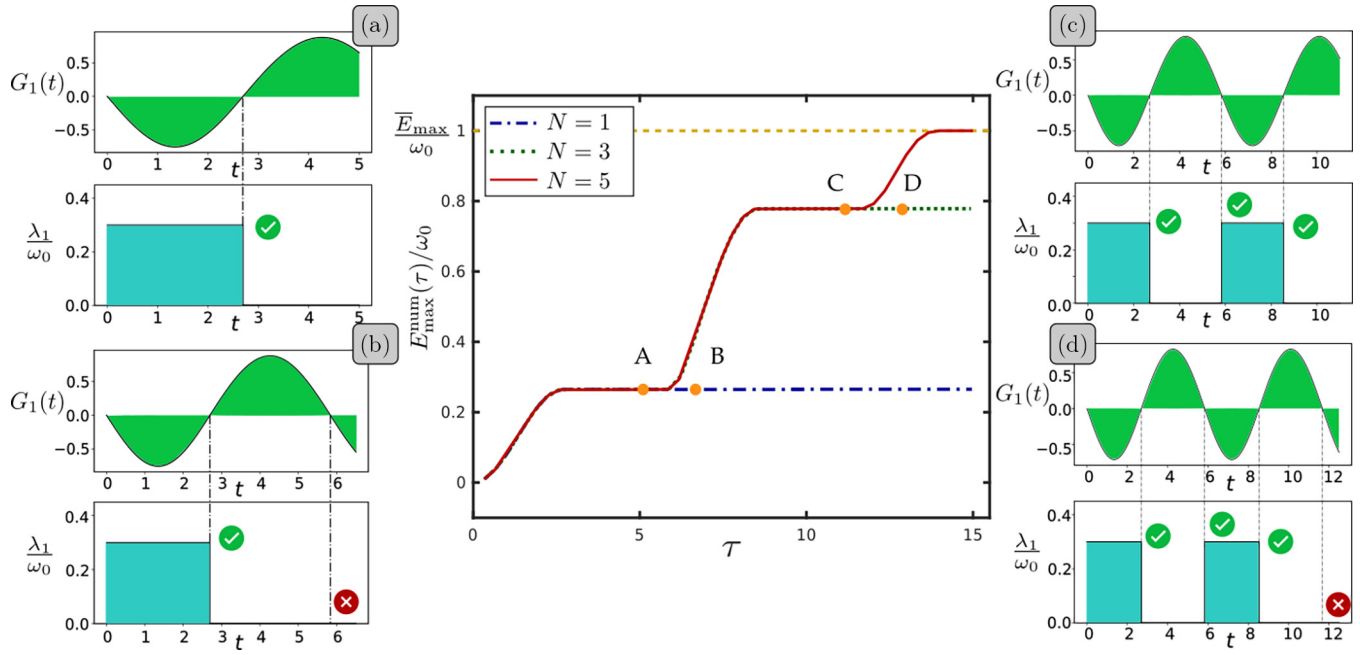

FIG. 4. Plot of the maximum-energy value $E_{\max}^{\text{num}}(\tau)$ at the end of DCP process (29) of duration τ, obtained by performing a numerical optimization with respect to the bang-bang protocols of Fig. 3 with different values of N [the charging term here is chosen such that $\boldsymbol{x} = (1, 0, 0)$]. The side panels report also the values of $\lambda_1(t)$ and of the associated $G_1(t)$ function computed as in Eq. (32) for four particular simulations. Notice that points A and C follow the PMP prescriptions detailed at the end of Sec. IV, while points B and D do not. More specifically, B and D miss the last switches, continuing to maintain $\lambda_1(t) = 0$: this happens because they have no possible switches left [we have fixed $N = 1$ and 3, respectively, and, consequently, they are forced to stay with $\lambda_1(t) = 0$ for the remaining time].

results with the PMP criteria. For this purpose we focused on four particular points A, B, C, and D of the central plot in Fig. 4. Each point corresponds to a particular charging protocol (i.e., N and Δt_1, $\Delta t_2, \ldots, \Delta t_{N+1}$ fixed) for which we present the explicit value of $\lambda_1(t)$ and the associated $G_1(t)$ function computed as in Eq. (32). We notice that only the protocols on the solid red line (i.e., A and C), which provide our best guess for the maximum final energy, fulfill the PMP criteria (a), (b), and (c) in Sec. IV A, that prescribe a switch of $\lambda_1(t)$ whenever $G_1(t)$ changes sign. The other two instead fail to follow the prescription, e.g., missing the final switching point. This is in line with the fact that B and D are clearly not optimal, since there are other points along the solid red line providing better final energy values for the same charging time τ.

Optimal charging times

We now tackle the problem of minimizing the charging time τ that enables us to reach a final target state $\rho_\diamond$. Integrating the equations of motion for $\rho(t)$ and $\pi(t)$ given in Sec. IV B we expressed them in the Bloch vector representation:

$$\rho(t) = \frac{\mathbb{1} + \boldsymbol{a}(t)\cdot\boldsymbol{\sigma}}{2},$$
$$\pi(t) = \frac{b_0\mathbb{1} - \boldsymbol{b}(t)\cdot\boldsymbol{\sigma}}{2}, \tag{38}$$

where at variance with (31) we parametrized the costate in a such a way to leave its trace undetermined and not directly connected with the length of the vector $\boldsymbol{b}(t)$. Replacing this into (26) we hence get

$$G_1(t) = \frac{i}{4}\,\langle \boldsymbol{b}(t)\cdot\boldsymbol{\sigma}[\boldsymbol{x}\cdot\boldsymbol{\sigma}, \boldsymbol{a}(t)\cdot\boldsymbol{\sigma}]\rangle \quad = \boldsymbol{x}\cdot\boldsymbol{b}(t)\wedge\boldsymbol{a}(t), \tag{39}$$

which up to an irrelevant scaling factor ω_0 coincides with the one given in Eq. (32). We can hence apply the same analysis of the previous section to declare that the optimal pulses will be again a piecewise-constant function belonging to the class (36) with the same set $\mathcal{S}$ of allowed constant plateaus (see Appendix B 1 for details).

B. Qubit optimal DCP with two charging fields ($m = 2$)

We now consider the charging process of a qubit in the presence of two controls. As in Sec. V A, we choose $H_0 = \frac{\omega_0}{2}(\mathbb{1} - \sigma_z)$ as reference Hamiltonian, but assume the presence of two different charging terms $H_1 = \sigma_x$ and $H_2 = \sigma_y$ with control functions $\lambda_1(t)$ and $\lambda_2(t)$ fulfilling a constraint which limits their joint intensity, i.e.,

$$\lambda_1^2(t) + \lambda_2^2(t) \leqslant r_{\max}^2, \tag{40}$$

that we can parametrize as $\lambda_1(t) := r(t)\cos\theta(t)$ and $\lambda_2(t) := r(t)\sin\theta(t)$ with $r(t) \in [0, r_{\max}]$ and $\theta(t)$ real. In this case we find it useful to study the problem using the interaction picture where, given $V(t) := e^{-iH_0 t}$, the unitary associated with the free evolution, we replace $\rho(t)$ with the density operator $\tilde{\rho}(t) := V(t)^\dagger\rho(t)V(t) = [\mathbb{1} + \tilde{\boldsymbol{a}}(t)\cdot\boldsymbol{\sigma}]/2$, with $\tilde{\boldsymbol{a}}(t)$ being its associated Bloch vector. Accordingly the dynamical equation of the model reads

$$\dot{\tilde{\rho}}(t) = -i[\tilde{H}_{\rm int}(t), \tilde{\rho}(t)] \iff \dot{\tilde{\boldsymbol{a}}}(t) = 2\tilde{\boldsymbol{\lambda}}(t)\wedge\tilde{\boldsymbol{a}}(t), \tag{41}$$

where

$$\tilde{H}_{\rm int}(t) := V(t)^\dagger[r(t)\cos\theta(t)\sigma_x + r(t)\sin\theta(t)\sigma_y]V(t)$$
$$= \tilde{\boldsymbol{\lambda}}(t)\cdot\boldsymbol{\sigma} \tag{42}$$

is the interaction picture Hamiltonian characterized by a control vector $\tilde{\boldsymbol{\lambda}}(t) = (\tilde{\lambda}_1(t), \tilde{\lambda}_2(t), 0)$ of components $\tilde{\lambda}_1(t) := r(t)\cos\tilde{\theta}(t)$ and $\tilde{\lambda}_2(t) := r(t)\sin\tilde{\theta}(t)$ with $\tilde{\theta}(t) := \theta(t) + \omega_0 t$. Noting that the final energy of the system still reads as

$$E(\tau) = \langle\tilde{\rho}(\tau)H_0\rangle, \tag{43}$$

we can cast the PMP using an associated costate $\tilde{\pi}'(t) = -\omega_0[\mathbb{1} + \tilde{\boldsymbol{b}}(t)\cdot\boldsymbol{\sigma}]/2$, which evolves via the same dynamical equation $\tilde{\rho}(t)$, i.e.,

$$\dot{\tilde{\pi}}'(t) = -i[\tilde{H}_{\rm int}(t), \tilde{\pi}'(t)] \iff \dot{\tilde{\boldsymbol{b}}}(t) = 2\tilde{\boldsymbol{\lambda}}(t)\wedge\tilde{\boldsymbol{b}}(t), \tag{44}$$

and a two-dimensional vector $\tilde{\boldsymbol{G}}(t)$ for the corresponding pseudo-Hamiltonian (20) that can be expressed as

$$\tilde{G}_j(t) := \omega_0\,\hat{\boldsymbol{x}}_j\cdot\tilde{\boldsymbol{b}}(t)\wedge\tilde{\boldsymbol{a}}(t), \quad \forall j = 1, 2 \tag{45}$$

with $\hat{\boldsymbol{x}}_1 = (1, 0, 0)$ and $\hat{\boldsymbol{x}}_2 = (0, 1, 0)$. Dropping the irrelevant constant factor ω_0, we can then cast the third PMP inequality of (22) as

$$\tilde{\boldsymbol{\lambda}}^\star(t)\cdot\tilde{\boldsymbol{b}}(t)\wedge\tilde{\boldsymbol{a}}(t) \leqslant \tilde{\boldsymbol{\lambda}}(t)\cdot\tilde{\boldsymbol{b}}(t)\wedge\tilde{\boldsymbol{a}}(t). \tag{46}$$

Solving Eq. (46) is much more demanding than the corresponding case with a single control function, so we will adopt a different strategy by guessing the optimal solution and after verifying that it fulfills the necessary conditions (46). Since $E(\tau) = \omega_0[1 - \tilde{a}_3(\tau)]/2$ we notice that increasing $E(\tau)$ is equivalent to decreasing the value of $\tilde{a}_3(\tau)$. In view of this fact we expect the maximum charging power to be achieved when $\boldsymbol{\lambda}(t)$ is chosen in order to force a rotation of the system (in the interaction picture) around the axis orthogonal to the plane containing the z axis and the Bloch vector $\boldsymbol{a}(0)$ [note that $\boldsymbol{a}(0)$ and $\tilde{\boldsymbol{a}}(0)$ coincide]. This axis is

$$\hat{\boldsymbol{k}} := \hat{\boldsymbol{x}}_3\wedge\boldsymbol{a}(0)/|\boldsymbol{a}(0)| = (\cos\theta_0, \sin\theta_0, 0), \tag{47}$$

with the implicit convention that if $\boldsymbol{a}(0)$ is oriented along the $\hat{\boldsymbol{x}}_3$ axis we then take $\hat{\boldsymbol{k}} = (1, 0, 0)$ (any other vector orthogonal to $\hat{\boldsymbol{x}}_3$ would work as well in this case). To achieve this we need $\tilde{\theta}(t) = \theta_0$ that is realized with the choice

$$\theta(t) = -\omega_0 t + \theta_0, \quad r(t) = r_{\max}, \tag{48}$$

where with the second condition we aim at maximizing the speed of rotation. When (48) holds we have $\tilde{H}_{\rm int}(t) = r_{\max}\hat{\boldsymbol{k}}\cdot\boldsymbol{\sigma}$ and the dynamical equation simply reads

$$\tilde{\boldsymbol{a}}(t) = \boldsymbol{a}(0)\cos(2r_{\max}t) + [\hat{\boldsymbol{k}}\wedge\boldsymbol{a}(0)]\sin(2r_{\max}t)$$
$$= |\boldsymbol{a}(0)\big[\cos(2r_{\max}t + \alpha_0)\hat{\boldsymbol{x}}_3 - \sin(2r_{\max}t + \alpha_0)(\hat{\boldsymbol{x}}_3\wedge\hat{\boldsymbol{k}})\big], \tag{49}$$

where in the second identity we used (47) and introduced the symbol

$$\alpha_0 := \arccos\left(\frac{\boldsymbol{a}(0)\cdot\hat{\boldsymbol{x}}_3}{|\boldsymbol{a}(0)|}\right) = \arccos a_3(0) \in [0, \pi], \tag{50}$$

to indicate the angle between the vectors $\boldsymbol{a}(0)$ and $\hat{\boldsymbol{x}}_3$. Accordingly we can write $\tilde{a}_3(t) = \boldsymbol{x}_3 \cdot \tilde{\boldsymbol{a}}(t) = |\boldsymbol{a}(0)| \cos(2r_{\max}t + \alpha_0)$, so that

$$E(\tau) = \omega_0[1 - |\boldsymbol{a}(0)| \cos(2r_{\max}t + \alpha_0)]/2. \tag{51}$$

Notice now that for t equal to $\tau_1 := (\pi - \alpha_0)/(2r_{\max})$ the function (51) reaches its maximum absolute value, i.e., $\overline{E}_{\max} := \omega_0 \frac{1+|\boldsymbol{a}(0)|}{2}$. We can hence identify two possible scenarios.

(1) If $\tau \geqslant \tau_1$ the optimal protocol is arguably to do a "pi pulse" and keep evolving the system using Eq. (48) until $t = \tau_1$, and then stopping, i.e.,

$$\tilde{\boldsymbol{\lambda}}^{\star}(t) = \begin{cases} r_{\max}\hat{\boldsymbol{k}} & \forall t \in [0, \tau_1], \\ 0 & \forall t \in]\tau_1, \tau], \end{cases} \tag{52}$$

with an associated final maximal energy $E(\tau)$ that saturates to the absolute maximum $\overline{E}_{\max}$.

(2) If $\tau < \tau_1$, our best candidate for the optimal protocol is to use (48) until the very end of the charging period, i.e.,

$$\tilde{\boldsymbol{\lambda}}^{\star}(t) = r_{\max}\hat{\boldsymbol{k}}, \quad \forall t \in [0, \tau], \tag{53}$$

with an associated optimal final energy that can be estimated as

$$E_{\max}(\tau) = \omega_0 \left[\frac{1 - |\boldsymbol{a}(0)| \cos(2r_{\max}\tau + \alpha_0)}{2} \right]. \tag{54}$$

We finally checked (see Appendix C for the details) that the above guesses verify the constraint Eq. (46). To conclude, it is interesting to compare the energy achieved with the optimal protocol in the $m = 2$ case with its analog in the $m = 1$ case (discussed in Sec. V A), thus highlighting the advantage of an increased accessible domain for the charging Hamiltonians. In Fig. 5 we plot the final energy in Eq. (54), picking $r_{\max} = 0.3\omega_0$, for different values of the total charging time τ and initializing the system in the ground state. In addition, we plot the correspondent quantity $E_{\max}(\tau)$ related to the case of only one control field ($m = 1$) treated in Sec. V A and an alternative $m = 1$ case in which we allow the intensity of the control to be negative. As expected, the latter two cases are subperforming with respect to the $m = 2$ case.

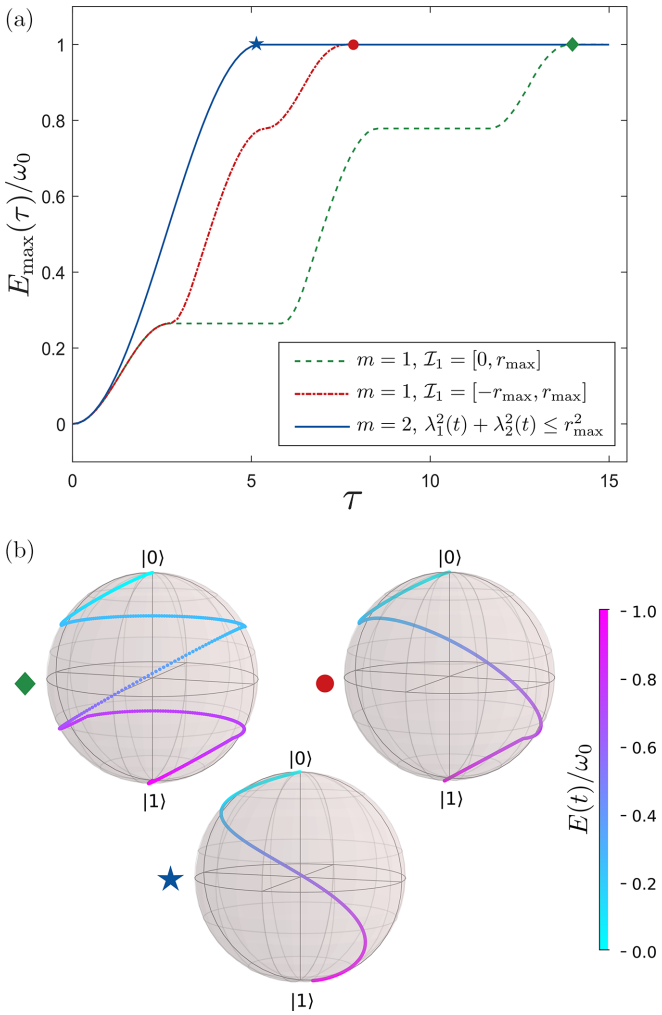

FIG. 5. Comparison of optimal charging processes for three different DCP models corresponding to different constraints on the controls (see legend). (a) The maximum-energy value at the end of a charging process of duration τ, where we have set $r_{\max} = 0.3\omega_0$. (b) The evolution in Bloch's sphere of a full charging process for all the different DCP models. In particular, each Bloch's sphere represents a specific instance of the optimal charging processes displayed in panel (a) (represented by a green diamond, a red circle, and a blue star).

C. Harmonic oscillator optimal charging

Here we analyze a DCP model for a continuous variable system with a single excitation mode described by the usual Hamiltonian (1), with a single control function ($m = 1$) and

$$H_0 = \omega_0 a^{\dagger}a, \quad H_1 = a + a^{\dagger}, \tag{55}$$

where $a^{\dagger}$ (a) is the creation (destruction) bosonic operator. As for the qubit DCP model of Sec. V A, we are interested in finding the optimal function $\lambda_1^{\star}(t)$, with $\lambda_1^{\min} \leqslant \lambda_1(t) \leqslant \lambda_1^{\max}$ as a constraint, that enforces an evolution that maximizes the energy of the system in a fixed time τ. In this case instead of solving the dynamical evolution in the standard Schrödinger picture we find it useful to adopt the Heisenberg representation. The reason for such a choice is that the expectation values of the first and second momenta of the field operator form a closed system of differential equations, i.e.,

$$\begin{array}{l} v_1(t) = \langle a^{\dagger}a\rho(t)\rangle \\ v_2(t) = \mathrm{Im}\,\langle a\rho(t)\rangle \\ v_3(t) = \mathrm{Re}\,\langle a\rho(t)\rangle \end{array} \Rightarrow \begin{cases} \dot{v}_1(t) = -2\lambda_1(t)v_2(t), \\ \dot{v}_2(t) = -\omega_0 v_3(t) - \lambda_1(t), \\ \dot{v}_3(t) = \omega_0 v_2(t), \end{cases} \tag{56}$$

with the cost function (18) expressed as

$$J = -\omega_0 \int_0^{\tau} \dot{v}_1(t)\, dt. \tag{57}$$

Notice that Eq. (56) represents the equation of motion of a classical harmonic oscillator driven by an external time-dependent force proportional to $\lambda_1(t)$, and Eq. (57) is proportional to the energy of the classical oscillator. Indeed, denoting with $r(t)$ and $v(t)$ the position and velocity of a particle of mass m coupled to a spring characterized by $k = m\omega_0^2$, the second equation of (56) can be written

as $m\dot{v}(t) = -kr(t) + F(t)$ through the identification $v_2(t) = \omega_0^{-1} v(t)$, $v_3(t) = r(t)$, and $\lambda_1(t) = -(m\omega_0)^{-1} F(t)$, with the third equation on the power of the battery being proportional to the power of the classical harmonic oscillator, i.e., $\dot{E}(t) = 2(m\omega_0)^{-1} v(t) F(t)$.

We now turn to the optimal control setting. We define the pseudo-Hamiltonian as in Eq. (11):

$$\mathcal{H} = 2\omega_0 \lambda_1(t) v_2(t) + p_1(t)[-2\lambda_1(t) v_2(t)] + p_2(t)[-\omega_0 v_3(t) - \lambda_1(t)] + p_3(t)[\omega_0 v_2(t)], \quad (58)$$

where the $p_i(t)'$s are the costates that enforce the evolution of the first and second momenta. Notice that as we are still in the case where $\mathcal{H}$ is linear in the control function $\lambda_1(t)$, the PMP inequality (12) is still of the form (22)

$$\lambda_1^\star(t) G_1(t) \leqslant \lambda_1(t) G_1(t), \quad (59)$$

with a single switching function:

$$G_1(t) = 2\omega_0 v_2(t) - 2p_1(t) v_2(t) - p_2(t). \quad (60)$$

As proved in Appendix D, when starting from the ground state of H_0, no singular intervals are allowed, leading to an optimal charging protocol consisting of a bang-bang modulation with $\lambda_1(t)$ switching between the values $\lambda_1^{\min}$ and $\lambda_1^{\max}$. In the long-time limit, this modulation achieves the optimal performance when its frequency is resonant with the one of the oscillator, as proven in Appendix E.

VI. EXAMPLES OF MCP MODELS

In this section we analyze MCPs where energy is transferred to the battery through an additional system (charger).

A. Qubit-qubit

We begin by studying the most straightforward case of a charger-battery setting with a single controllable interaction term ($m = 1$): here, the charger and the quantum battery are two qubits that evolve according to a global Hamiltonian of the form (7), with

$$\begin{aligned} H_A &= \frac{\omega_A}{2}\left(\mathbb{1} - \sigma_z^{\mathrm{A}}\right), \\ H_B &= \frac{\omega_B}{2}\left(\mathbb{1} - \sigma_z^{\mathrm{B}}\right), \\ H_1 &= (\sigma_+^{\mathrm{A}} + \sigma_-^{\mathrm{A}})(\sigma_+^{\mathrm{B}} + \sigma_-^{\mathrm{B}}), \end{aligned} \quad (61)$$

where $\sigma_{x,y,z}^{\mathrm{S}}$ are Pauli matrices acting on system $S = A, B$ and $\sigma_+^{\mathrm{S}} = [\sigma_-^{\mathrm{S}}]^\dagger = (\sigma_x^{\mathrm{S}} + i\sigma_y^{\mathrm{S}})/2$ is the two-level raising operator. Throughout this section, we focus on the $\omega_A \neq \omega_B$ case since the energy transfer trivially occurs via the well-known Rabi oscillations [4] when the two qubits are resonant ($\omega_A = \omega_B$). For general initial states, determining the optimal $\lambda_1(t)$ that leads to the maximum value for the final energy stored in the subsystem B is quite challenging, due to the fact that the evolution of the quantum battery in this setting is not unitary. However, we can exploit the fact that in the $\{|00\rangle, |11\rangle, |10\rangle, |01\rangle\}$ basis the resulting Hamiltonian (62) is a block-diagonal matrix:

$$H(t) = \begin{pmatrix} 0 & \lambda_1(t) & 0 & 0 \\ \lambda_1(t) & \omega_B + \omega_A & 0 & 0 \\ 0 & 0 & \omega_A & \lambda_1(t) \\ 0 & 0 & \lambda_1(t) & \omega_B \end{pmatrix}. \quad (62)$$

Accordingly, we can map the MCP model into a single-qubit DCP scheme by suitably choosing the initial state.

1. *Case* $\rho_{AB}(0) = |10\rangle\langle 10|$

We first consider the battery in the ground state and the charger completely charged, assuming as input state of the model $\rho_{AB}(0) = |10\rangle\langle 10|$. It is evident that in this situation we can consider just the second block in Eq. (62), associated with the basis $\{|10\rangle, |01\rangle\}$. Let us call our new vector basis as $|g\rangle := |10\rangle$ (for "ground state") and $|e\rangle := |01\rangle$ (for "excited state"). This is now equivalent to a single-qubit model with reference Hamiltonian

$$H'(t) := H_0' + \lambda_1(t) H_1', \quad (63)$$

where

$$\begin{aligned} H_0' &:= \tfrac{\omega_A+\omega_B}{2}\mathbb{1} + \tfrac{\omega_A-\omega_B}{2}\sigma_z = \omega_A |g\rangle\langle g| + \omega_B |e\rangle\langle e|, \\ H_1' &:= \sigma_x = |e\rangle\langle g| + |g\rangle\langle e|. \end{aligned} \quad (64)$$

The global state at time t can be written as $|\psi'(t)\rangle = \alpha(t)|g\rangle + \beta(t)|e\rangle$, corresponding to a reduced density matrix $\rho_B(t) = |\alpha(t)|^2 |0\rangle\langle 0| + |\beta(t)|^2 |1\rangle\langle 1|$ for the battery. The maximization of $E_B(\tau)$ can now be turned into a DCP problem by noting that

$$\begin{aligned} E_B(\tau) &= \langle \rho_B(\tau) H_B \rangle = |\beta(\tau)|^2 \omega_B \\ &= \langle \rho'(t) H_B' \rangle, \end{aligned} \quad (65)$$

with $H_B' := \omega_B |e\rangle\langle e|$. The original MCP has been turned into a modified single-qubit DCP problem, that is the same as the one presented in Sec. V A, apart from an additional term appearing in the energy function $H_B' = H_0' - H_A'$, where $H_A' = \omega_A |g\rangle\langle g|$. However, notice that the presence of H_A' does not change the nature of the optimal solutions, since the points where $E_B(\tau) = |\beta(\tau)|^2 \omega_B$ and $\langle \rho'(t) H_0' \rangle = \omega_A + |\beta(\tau)|^2(\omega_B - \omega_A)$ have extrema are the same (in more detail, a maximum of the former respectively corresponds to a maximum or minimum of the latter depending on the sign of $\omega_B - \omega_A$). With this in mind, we can still treat the problem using the same PMP approach we detailed in Sec. IV, writing the cost function as

$$J = -\int_0^\tau \langle H_B' \mathcal{N}[\rho'(t)] \rangle dt, \quad (66)$$

with $\mathcal{N}[\rho'(t)] = -i[H'(t), \rho'(t)]$. More precisely, the optimization problem is equivalent, with the following arrangements:

$$|0\rangle \to |g\rangle, \quad |1\rangle \to |e\rangle, \quad (67)$$

$$H_0 \to H_0', \quad H_1 \to H_1', \quad (68)$$

$$E(t) = \langle \rho(t) H_0 \rangle \to E_B(t) = \langle \rho'(t) H_B' \rangle. \quad (69)$$

Therefore, since $H_1' = \sigma_x$, we have shown in Sec. V A that the bang-bang-off protocol is the optimal choice for this initial configuration.

2. Case $\rho_{AB}(0) = |00\rangle\langle 00|$

We now consider a case where both the battery and the charger start in their ground state. The process is not a simple energy flow from one system to another since they start completely uncharged. Instead, the energy comes from the modulation of the interacting Hamiltonian H_1. The charger works more like a "plug" that allows the battery to absorb energy thanks to their interaction. Interestingly, thanks to the block structure of the global Hamiltonian (62), also this case can be mathematically mapped into a single-qubit battery with reference Hamiltonian as in (63), where

$$\begin{aligned} H_0' &= \tfrac{\omega_A+\omega_B}{2}\mathbb{1} - \tfrac{\omega_B+\omega_A}{2}\sigma_z, \\ H_1' &= \sigma_x. \end{aligned} \tag{70}$$

Therefore, the optimal charging with these initial conditions will still be performed through a bang-bang-off protocol.

B. Harmonic oscillator–qubit

In this section we want to understand if it is possible to boost the qubit charging process by considering a different charger, focusing on the analysis of a quantum harmonic oscillator system as a charger. Since we can have more than one excited level in this case, we expect that fixing the same frequency ω_A will allow us to charge our battery faster. We consider the global Hamiltonian of the system still in the form (7), with

$$H_A = \omega_A\, a^\dagger a, \quad H_B = \omega_B \frac{\mathbb{1} - \sigma_z}{2}, \tag{71}$$

$$H_1 = a^\dagger \sigma_- + a\sigma_+. \tag{72}$$

Considering as initial state $\rho_{AB}(0) = |n, 0\rangle\langle n, 0|$, that is, the charger is prepared in an eigenvector of the number operator $a^\dagger a$ with eigenvalue n, and the battery is initialized in the ground state, we can restrict the analysis to subspaces with a given number n of excitations spanned by vectors $|g\rangle = |n, 0\rangle$ and $|e\rangle = |n-1, 1\rangle$. The Hamiltonian contributions in this two-dimensional subspace are

$$\begin{aligned} H_0' &= \left[\tfrac{\omega_A(2n-1)+\omega_B}{2}\right]\mathbb{1} + \left(\tfrac{\omega_A-\omega_B}{2}\right)\sigma_z, \\ H_1' &= \sqrt{n}\sigma_x. \end{aligned} \tag{73}$$

This is equivalent to the qubit-qubit case in Eq. (64) by changing $\lambda^{\max} \to \sqrt{n}\lambda^{\max}$ (the coefficient that multiplies the identity operator is always irrelevant). Consequently, we are boosting the bang-bang-off protocol, allowing us to charge the qubit battery faster than the two-qubit protocol by a factor of $\sqrt{n}$.

VII. CONCLUSIONS

We have presented a systematic analysis of two quantum battery charging processes, focusing on qubit systems and quantum harmonic oscillators. We analyzed two charging scenarios: (1) the direct charging process, where a single quantum system, representing the battery, is charged through the modulation of an external Hamiltonian, and (2) the mediated charging process, where energy is transferred between two quantum systems A and B, representing respectively the charger and battery.

We have shown that the optimal charging protocols for both approaches are obtained by modulating the control parameter as a step function between few specific values, greatly simplifying the optimal control problem. In particular, we observed that alternating the intensity of the control parameter between its boundary limits is almost always an optimal strategy.

We have also shown that replacing the qubit charger with a quantum harmonic oscillator can enhance the performance of our charging process, allowing us to charge the battery faster. This result was expected since we can store more energy in a quantum harmonic oscillator system with the same frequency. This inevitably has a positive impact on the charging protocol, as encountered in our analysis.

A natural direction for future research is extending this analysis to the case of open quantum systems, where a unitary operation no longer describes the state evolution. In addition, it would be interesting to exploit our control methods with scalable many-body systems. We know already from our analysis in Sec. IV A that a charging DCP model of a many-body battery with one control will likely result in an optimal bang-bang modulation (or a possible variant depending on the singular intervals). Moreover, building on the work presenting a $\sqrt{N}$ speedup in the collective charging of a so-called Dicke quantum battery [13], i.e., a particular MCP model where N qubits are coupled to a single cavity in a resonant regime, our model could be used to extend that result to a more general scenario (for example by considering both a nonzero detuning and a time-dependent control).

ACKNOWLEDGMENTS

F.M. acknowledges support by the European Union's Quantum Technology Flagship, through the Horizon 2020 research and innovation program, under CIVIQ Grant No. 820466 and OPENQKD Grant No. 857156. V.C. is supported by the Luxembourg national research fund in the framework of project QUTHERM (Grant No. C18/MS/12704391). P.A.E. gratefully acknowledges funding by the Berlin Mathematics Center MATH + (AA1-6, AA2-18). V.G. acknowledges financial support by Ministero dell'Istruzione, Università e della Ricerca via PRIN 2017 "Taming complexity via Quantum Strategies: a Hybrid Integrated Photonic approach (QUSHIP)" (Grant No. 2017SRN-BRK), and via project PRO3 "Quantum Pathfinder."

APPENDIX A: ERGOTROPY, TOTAL ERGOTROPY, AND THERMAL FREE ENERGY

At variance with purely classical settings, discriminating which part of the internal energy of a quantum system ρ can be identified with extractable work is difficult [49,53–55]. Ergotropy $\mathcal{E}[\rho, H]$, total ergotropy $\mathcal{E}_{\text{tot}}[\rho, H]$, and thermal free energy $\mathcal{F}_{\tilde{\beta}}[\rho, H]$ are three different ways to evaluate such a quantity based on different assumptions on the resources we have dedicated to the task. The first one measures the amount of work we can get from ρ if we limit the allowed

operations to local unitary transformations. Formally it can be expressed as

$$\mathcal{E}[\rho, H] := \langle \rho H \rangle - \min_{U\in\mathcal{U}} \langle U\rho U^\dagger H\rangle, \tag{A1}$$

where the minimization in the first term is performed over all possible unitary transformations acting on the system. Such a term can be cast in a closed formula by introducing the passive counterpart $\rho^\downarrow$ of ρ [56,57], i.e., the special state which has the lowest energy among those with the same spectrum of ρ. Introducing the spectral decomposition $\rho = \sum_i \eta_i |i\rangle\langle i|$ and $H = \sum_i \epsilon_i |\epsilon_i\rangle\langle\epsilon_i|$ of the state and of the Hamiltonian, we can write

$$\rho^\downarrow := \sum_i \eta_i^\downarrow |\epsilon_i^\uparrow\rangle\langle\epsilon_i^\uparrow|, \tag{A2}$$

where $s_\rho^\downarrow := \{\eta_1^\downarrow, \eta_2^\downarrow, \ldots\}$ is a rearrangement of the spectrum $s_\rho := \{\eta_1, \eta_2, \ldots\}$ of ρ where the various terms are organized in decreasing order (i.e., $\eta_i^\downarrow \geqslant \eta_i^\downarrow$), and $\{|\epsilon_i^\uparrow\rangle\}_i$ are instead the eigenvectors of the system Hamiltonian organized in increasing order of their associated eigenvalues (i.e., $\epsilon_i^\uparrow \leqslant \epsilon_{i+1}^\uparrow$). With this choice Eq. (A1) can hence be written as

$$\mathcal{E}[\rho, H] = \langle \rho H\rangle - \langle \rho^\downarrow H\rangle = \langle \rho H\rangle - \sum_i \eta_i^\downarrow \epsilon_i^\uparrow, \tag{A3}$$

which applied to our problem leads to Eq. (6) with $\mathcal{F}(s_{\rho(t)}, s_{H_t}) = \mathcal{F}(s_{\rho(0)}, s_{H_0}) = \sum_i \eta_i^\downarrow(0)\, \epsilon_i^\uparrow(0)$. It is worth noticing that a quantity that is related to $\mathcal{E}[\rho, H]$ is the antiergotropy functional $\mathcal{A}[\rho, H]$ that instead gauges the minimum work extractable from the system via unitary transformations [50]. This is obtained by replacing the minimization in Eq. (A1) with a maximization, i.e.,

$$\begin{aligned}\mathcal{A}[\rho, H] &:= \langle \rho H\rangle - \max_{U\in\mathcal{U}} \langle U\rho U^\dagger H\rangle \\ &= \langle \rho H\rangle - \langle \rho^\uparrow H\rangle = \langle \rho H\rangle - \sum_i \eta_i^\uparrow \epsilon_i^\uparrow,\end{aligned} \tag{A4}$$

where now $\rho^\uparrow := \sum_i \eta_i^\uparrow |\epsilon_i^\uparrow\rangle\langle\epsilon_i^\uparrow|$ is the antipassive counterpart of ρ.

Ergotropy turns out to be nonextensive [58,59]: when operating with reversible coherent operations on N copies of a given state ρ, it is possible to increase the total amount of extractable energy by acting jointly on the whole set of subsystems. The maximum amount of energy per copy that is attainable under this new paradigm is quantified by the *total ergotropy* $\mathcal{E}_{\rm tot}[\rho, H]$, a functional which can obtained via a proper regularization of (A1), i.e.,

$$\begin{aligned}\mathcal{E}_{\rm tot}[\rho, H] &:= \lim_{n\to\infty} \frac{1}{n} \mathcal{E}[\rho^{\otimes n}, H^{(n)}] = \langle \rho H\rangle - \langle \tau_\beta H\rangle \\ &= \langle \rho H\rangle - \frac{\sum_i e^{-\beta\epsilon_i}\epsilon_i}{\sum_i e^{-\beta\epsilon_i}},\end{aligned} \tag{A5}$$

where $\tau_\beta := e^{-\beta H}/{\rm Tr}[e^{-\beta H}]$ is a thermal Gibbs state of the system whose inverse temperature $\beta \in \mathbb{R}^+$ is fixed in order to ensure that it possesses the same von Neumann entropy of ρ, i.e.,

$$S(\tau_\beta) = S(\rho) := -{\rm Tr}[\rho \log \rho] = -\sum_i \eta_i \log \eta_i. \tag{A6}$$

Notice that as β is an implicit function of just the spectrum of ρ, we can again cast the total ergotropy as in Eq. (6) by setting $\mathcal{F}(s_{\rho(t)}, s_{H_t}) = \mathcal{F}(s_{\rho(0)}, s_{H_0}) = \langle \tau_{\beta_0} H_0\rangle$ with $\beta_0 = \beta(s_{\rho(0)})$.

Finally beyond the value defined by $\mathcal{E}_{\rm tot}[\rho, H]$ more energy from the system can still be converted into useful work only if we are willing to admit some dissipation side effect, e.g., by coupling the system with an external thermal bath [49,60]. In this case the overall amount of extractable energy is provided by the nonequilibrium free-energy functional:

$$\mathcal{F}_{\bar\beta}[\rho, H] := \langle \rho H\rangle - S(\rho)/\bar\beta = \langle \rho H\rangle + (1/\bar\beta)\sum_i \eta_i \log \eta_i, \tag{A7}$$

with $\bar\beta$ representing the inverse temperature of the bath. Once more, for our problem the above expression reduces to the form of Eq. (6): $\mathcal{F}(s_{\rho(0)}, s_{H_0}) = (1/\bar\beta)\sum_i \eta_i(0)\log\eta_i(0)$.

APPENDIX B: SINGULAR INTERVAL ANALYSIS FOR THE DCP QUBIT MODEL WITH A SINGLE CONTROL FUNCTION

We have shown in Sec. V A that for the DCP qubit model with a single control function having singular intervals ($G_1(t) = 0$) is equivalent to having $\boldsymbol{x}\cdot\boldsymbol{b}(t) \wedge \boldsymbol{a}(t) = 0$ [see Eq. (33)]. A closed inspection of this formula implies that there are only two alternatives allowed: (1) $\boldsymbol{x} \perp \boldsymbol{a}(t) \wedge \boldsymbol{b}(t)$ and (2) $\boldsymbol{a}(t) \parallel \boldsymbol{b}(t)$, with $\boldsymbol{x}$ the three-dimensional (3D) vector which defines the charging Hamiltonian (29), and with $\boldsymbol{a}(t)$ and $\boldsymbol{b}(t)$ the Bloch vectors (31) which define the temporal evolution of the state and of the costate of the system (29). In the following we shall analyze separately the two cases, showing that the only possible option one has is provided by condition (34) of the main text.

1. Condition 1

Enforcing condition 1 for some nontrivial temporal interval requires that in such an interval $\boldsymbol{a}(t)$ and $\boldsymbol{b}(t)$ remain in the the plane orthogonal to the vector $\boldsymbol{x}$. Rewriting the system Hamiltonian in the Bloch vector form,

$$H(t) = H_0 + \lambda_1(t) H_1 = \boldsymbol{n}(t)\cdot\boldsymbol{\sigma}, \tag{B1}$$

with $\boldsymbol{n}(t)$ the row vector

$$\boldsymbol{n}(t) := 2(x_1\lambda_1(t), x_2\lambda_1(t), x_3\lambda_1(t) - \omega_0/2), \tag{B2}$$

reveals that the dynamics (22) forces both $\boldsymbol{a}(t)$ and $\boldsymbol{b}(t)$ to undergo rotations around the time-dependent axis (B2) evaluated on the optimal control $\lambda_1^\star(t)$, i.e.,

$$\begin{aligned}\dot{\boldsymbol{a}}(t) &= \langle \boldsymbol{\sigma}\dot\rho(t)\rangle = -i\langle \boldsymbol{\sigma}[\boldsymbol{n}^\star(t)\cdot\boldsymbol{\sigma}, \rho(t)]\rangle = \boldsymbol{n}^\star(t)\wedge\boldsymbol{a}(t), \\ \dot{\boldsymbol{b}}(t) &= -\tfrac{1}{\omega_0}\frac{\langle\boldsymbol{\sigma}\dot\pi'(t)\rangle}{\omega_0} = \tfrac{i}{\omega_0}\langle\boldsymbol{\sigma}[\boldsymbol{n}^\star(t)\cdot\boldsymbol{\sigma}, \pi'(t)]\rangle \\ &= \boldsymbol{n}^\star(t)\wedge\boldsymbol{b}(t),\end{aligned} \tag{B3}$$

with

$$\boldsymbol{n}^\star(t) := \boldsymbol{n}(t)|_{\lambda_1(t)=\lambda_1^\star(t)}. \tag{B4}$$

A little algebra now reveals that condition 1 allows only one possible solution, i.e., taking $\boldsymbol{x}$ orthogonal to $\boldsymbol{n}^\star(t)$. To see this explicitly observe that by construction Eq. (B3) implies that

also the vector $\boldsymbol{c}(t) = \boldsymbol{a}(t) \wedge \boldsymbol{b}(t)$ and all its time derivatives undergo the same dynamics of $\boldsymbol{a}(t)$ and $\boldsymbol{b}(t)$, i.e.,

$$\begin{aligned}\dot{\boldsymbol{c}}(t) &= \boldsymbol{n}^\star(t) \wedge \boldsymbol{c}(t),\\ \ddot{\boldsymbol{c}}(t) &= \boldsymbol{n}^\star(t) \wedge \dot{\boldsymbol{c}}(t) = \boldsymbol{n}^\star(t) \wedge [\boldsymbol{n}^\star(t) \wedge \boldsymbol{c}(t)].\end{aligned} \tag{B5}$$

Now if we wish to enforce the orthogonality condition between $\boldsymbol{c}(t)$ and $\boldsymbol{x}$ for some finite time interval that implies in particular that the following conditions must hold:

$$\boldsymbol{x} \cdot \boldsymbol{c}(t) = 0, \tag{B6}$$

$$\boldsymbol{x} \cdot \dot{\boldsymbol{c}}(t) = \boldsymbol{x} \cdot \boldsymbol{n}^\star(t) \wedge \boldsymbol{c}(t) = 0, \tag{B7}$$

$$\boldsymbol{x} \cdot \ddot{\boldsymbol{c}}(t) = \boldsymbol{x} \cdot \boldsymbol{n}^\star(t) \wedge [\boldsymbol{n}^\star(t) \wedge \boldsymbol{c}(t)] = 0, \tag{B8}$$

i.e., we need to choose $\boldsymbol{x}$ in such a way that it is orthogonal to $\boldsymbol{c}(t)$, $\boldsymbol{c}_1(t) := \boldsymbol{n}^\star(t) \wedge \boldsymbol{c}(t)$, and $\boldsymbol{c}_2(t) := \boldsymbol{n}^\star(t) \wedge [\boldsymbol{n}^\star(t) \wedge \boldsymbol{c}(t)]$ at the same time. Since all these vectors live in a 3D space, the only possibility we have to fulfill such a constraint is when $\boldsymbol{c}(t)$, $\boldsymbol{c}_1(t)$, and $\boldsymbol{c}_2(t)$ are not linearly independent. Consider first the scenario where $\boldsymbol{n}^\star(t)$ is parallel to $\boldsymbol{c}(t)$: in this case $\boldsymbol{c}_1(t) = \boldsymbol{c}_2(t) = 0$ and the last two conditions of (B6)–(B8) trivialize. A solution of condition 1 can be hence obtained by forcing orthogonality between $\boldsymbol{x}$ and $\boldsymbol{n}^\star(t)$, i.e.,

$$\boldsymbol{x} \cdot \boldsymbol{n}^\star(t) = 2\lambda_1^\star(t) - \omega_0 x_3 = 0, \tag{B9}$$

leading to condition (34) of the main text. Consider next the case where instead $\boldsymbol{n}^\star(t)$ is orthogonal to $\boldsymbol{c}(t)$: in this case $\boldsymbol{n}^\star(t)$, $\boldsymbol{c}(t)$, and $\boldsymbol{c}_1(t)$ will form an orthogonal set, forcing $\boldsymbol{c}_2(t)$ to be parallel to $\boldsymbol{c}(t)$. In other words if $\boldsymbol{n}^\star(t)$ is orthogonal to $\boldsymbol{c}(t)$, then $\boldsymbol{c}(t)$, $\boldsymbol{c}_1(t)$, and $\boldsymbol{c}_2(t)$ lay on a plane which is orthogonal to $\boldsymbol{n}^\star(t)$ and one could satisfy the conditions (B6)–(B8) by simply choosing $\boldsymbol{x}$ parallel to $\boldsymbol{n}^\star(t)$. However, as evident from (B2), the only case where we can have $\boldsymbol{x} \parallel \boldsymbol{n}^\star(t)$ is when $\omega_0 = 0$, which is not included in our analysis. Finally we are left with the intermediate case where $\boldsymbol{n}^\star(t)$ is neither orthogonal nor parallel to $\boldsymbol{c}(t)$: in this scenario we shall have that $\boldsymbol{c}(t)$, $\boldsymbol{c}_1(t)$, and $\boldsymbol{n}^\star(t)$ will be independent but will not form a mutually orthogonal set. Therefore in this case $\boldsymbol{c}_2(t)$ is not forced to be in the plane spanned by $\boldsymbol{c}(t)$ and $\boldsymbol{c}_1(t)$, making them linearly independent: no solutions of (B6)–(B8) can be found in this case.

2. Condition 2

Consider next the case of condition 2: since the state $\rho(t)$ and the costate $\pi'(t)$ obey the same evolution, once their Bloch vectors $\boldsymbol{a}(t)$ and $\boldsymbol{b}(t)$ become parallel, they will continue to be parallel for all the remaining time of the protocol. This means that we can equivalently check the condition at the final time τ, rewriting it as

$$\boldsymbol{a}(\tau) \parallel \boldsymbol{b}(\tau) = (0, 0, -1), \tag{B10}$$

where we used the fact that $\pi'(\tau) = -H_0$. This implies that condition 2 can only be realized if $\boldsymbol{a}(\tau) = \pm|\boldsymbol{a}|\ (0, 0, 1)$, What we have proved is that, to be in a singular interval, the state has to reach either the minimum energy achievable with a unitary evolution or the maximum one. The first option is certainly undesirable for an optimal control method, since it does not lead to an optimal protocol, and for this reason we discard it. However, the second option would surely be the best protocol.

3. Singular interval analysis for the time-optimization problem

As seen in Sec. V A, when optimizing the charging time for fixed final state $\rho_\diamond$ the switching function $G_1(t)$ has the same structure of the maximum-energy optimization problem [see Eq. (39)], the only difference being with the specific values of the vectors $\boldsymbol{a}(t)$ and $\boldsymbol{b}(t)$ which arise from dynamical equations which in principle are different from those of Eq. (33). Imposing the singular interval condition for $G_1(t)$ we hence get the same two possibilities detailed at the beginning of Sec. VII. Condition 1 leads exactly to the identification of the same condition (34); indeed also here we can rely on the fact that both $\boldsymbol{a}(t)$ and $\boldsymbol{b}(t)$ rotate around a common axis $\boldsymbol{n}^\star(t)$.

Condition 2 requires however an independent analysis as now (B10) does not hold. Instead we can invoke the constraint (28) which expressed in terms of the controls of the DCP problem becomes

$$i = \langle \pi(\tau)[H(\tau), \rho_\diamond]\rangle = \tfrac{1}{4}\langle H(\tau)[\boldsymbol{a}_\diamond \cdot \boldsymbol{\sigma}, \boldsymbol{b}(\tau) \cdot \boldsymbol{\sigma}]\rangle, \tag{B11}$$

with $\boldsymbol{a}_\diamond$ being the Bloch vector of the target state $\rho_\diamond$. Observe next that the following identity applies:

$$\begin{aligned}[\boldsymbol{a}_\diamond \cdot \boldsymbol{\sigma}, \boldsymbol{b}(\tau) \cdot \boldsymbol{\sigma}] &= [\boldsymbol{a}(\tau) \cdot \boldsymbol{\sigma}, \boldsymbol{b}(\tau) \cdot \boldsymbol{\sigma}]\\ &= -4[\rho(\tau), \pi(\tau)]\\ &= -4U_\tau^\star (U_t^\star)^\dagger [\rho(t), \pi(t)] U_t^\star (U_\tau^\star)^\dagger\\ &= U_\tau^\star (U_t^\star)^\dagger [\boldsymbol{a}(t) \cdot \boldsymbol{\sigma}, \boldsymbol{b}(t) \cdot \boldsymbol{\sigma}] U_t^\star (U_\tau^\star)^\dagger,\end{aligned} \tag{B12}$$

for all $t \in [0, \tau]$ and where we defined $U_t^\star := \mathcal{T} \exp[-i \int_0^t dt' H^\star(t')]$. The first of equalities (B12) is a consequence of the constraint $\rho(\tau) = \rho_\diamond$, the second and the fourth derive from the Bloch representation of the state and of the costate, and the third derives from the unitarity of the evolution. It is hence clear that if we do have a case where $\boldsymbol{a}(t)$ is parallel to $\boldsymbol{b}(t)$ for some time t, then $[\boldsymbol{a}(t) \cdot \boldsymbol{\sigma}, \boldsymbol{b}(t) \cdot \boldsymbol{\sigma}] = 0$, leading to a contradiction when replaced into (B11). This means that for the time optimization problem, enforcing condition 2 to identify the presence of singular time intervals always leads to a contradiction: Eq. (34) is the only option that we have.

APPENDIX C: PMP ANALYSIS FOR THE QUBIT DCP WITH TWO CHARGING FIELDS

Here we show that the solutions (52) and (53) fulfill the PMP condition (46).

Let us start by considering first the case (53) where during the entire charging interval $\tilde{\boldsymbol{\lambda}}^\star(t)$ maintains a constant value equal to $r_{\max}\hat{\boldsymbol{k}}$. By direct integration of Eq. (44) we get

$$\tilde{\boldsymbol{b}}(t) = \boldsymbol{b}_\parallel(0) + \boldsymbol{b}_\perp(0)\cos(2r_{\max}t) + [\hat{\boldsymbol{k}} \wedge \boldsymbol{b}_\perp(0)]\sin(2r_{\max}t), \tag{C1}$$

with $\boldsymbol{b}_\parallel(0)$ and $\boldsymbol{b}_\perp(0)$ the components of $\boldsymbol{b}(0)$ which are parallel and orthogonal to $\hat{\boldsymbol{k}}$, respectively. Notice however that since $\tilde{\pi}'(\tau) = -H_0$, we must have $\tilde{\boldsymbol{b}}(\tau) = (0, 0, -1) = -\hat{\boldsymbol{x}}_3$: replacing this into (C1) and remembering that $\hat{\boldsymbol{k}}$ is orthogonal to $\hat{\boldsymbol{x}}_3$ [see Eq. (47)], we can conclude that $\boldsymbol{b}_\parallel(0) = 0$. Hence

Eq. (C1) simplifies to

$$\begin{aligned}\tilde{\boldsymbol{b}}(t) &= \boldsymbol{b}(0)\cos(2r_{\max}t) + [\hat{\boldsymbol{k}}\wedge\boldsymbol{b}(0)]\sin(2r_{\max}t),\\ &= |\boldsymbol{b}(0)|[\cos(2r_{\max}t+\beta_0)\hat{\boldsymbol{x}}_3 - \sin(2r_{\max}t+\beta_0)(\hat{\boldsymbol{x}}_3\wedge\hat{\boldsymbol{k}})]\end{aligned} \tag{C2}$$

with

$$\beta_0 := \arccos\left(\frac{\boldsymbol{b}(0)\cdot\hat{\boldsymbol{x}}_3}{|\boldsymbol{b}(0)|}\right) = \arccos b_3(0) \in [0,\pi]. \tag{C3}$$

Comparing Eqs. (C2) and (49) reveals that for the entire dynamical evolution $\tilde{\boldsymbol{a}}(t)$ and $\tilde{\boldsymbol{b}}(t)$ lay on the plane orthogonal to $\hat{\boldsymbol{k}}$, rotating with the same constant angular velocity given by $r_{\max}$. In particular, this implies that their vectorial product is constant in time during the entire evolution and pointing into a direction which is antiparallel to the rotation axis $\hat{\boldsymbol{k}}$, i.e.,

$$\begin{aligned}\tilde{\boldsymbol{b}}(t)\wedge\tilde{\boldsymbol{a}}(t) &= \tilde{\boldsymbol{b}}(\tau)\wedge\tilde{\boldsymbol{a}}(\tau) = -\hat{\boldsymbol{x}}_3\wedge\tilde{\boldsymbol{a}}(\tau)\\ &= -|\boldsymbol{a}(0)|\sin(2r_{\max}\tau+\alpha_0)\,\hat{\boldsymbol{k}},\end{aligned} \tag{C4}$$

where we use (49) and the fact that $\hat{\boldsymbol{x}}_3\wedge(\hat{\boldsymbol{x}}_3\wedge\hat{\boldsymbol{k}}) = -\hat{\boldsymbol{k}}$ [notice that since $\tau\leqslant\tau_1$ we have that $2r_{\max}\tau+\alpha_0\leqslant\pi$ so that $\sin(2r_{\max}\tau+\alpha_0)\geqslant 0$]. From this Eq. (46) now follows by observing that

$$\begin{aligned}-\tilde{\boldsymbol{\lambda}}(t)\cdot\tilde{\boldsymbol{b}}(t)\wedge\tilde{\boldsymbol{a}}(t) &\leqslant |\tilde{\boldsymbol{\lambda}}(t)||\tilde{\boldsymbol{b}}(t)\wedge\tilde{\boldsymbol{a}}(t)|\\ &\leqslant r_{\max}|\boldsymbol{a}(0)|\sin(2r_{\max}\tau+\alpha_0)\\ &= -\tilde{\boldsymbol{\lambda}}^{\star}(t)\cdot\tilde{\boldsymbol{b}}(t)\wedge\tilde{\boldsymbol{a}}(t).\end{aligned} \tag{C5}$$

In the case described by Eq. (52) we are supposed to keep $\tilde{\boldsymbol{\lambda}}^{\star}(t)$ equal to $r_{\max}\hat{\boldsymbol{k}}$ for all $t\in[0,\tau_1]$ and then to switch off the control. This means that for all $t\in]\tau_1,\tau]$ both $\tilde{\boldsymbol{a}}(t)$ and $\tilde{\boldsymbol{b}}(t)$ are constant and equal to their final values, i.e.,

$$\begin{aligned}\tilde{\boldsymbol{a}}(t) &= \tilde{\boldsymbol{a}}(\tau) = -|\boldsymbol{a}(0)|\hat{\boldsymbol{x}}_3,\\ \tilde{\boldsymbol{b}}(t) &= \tilde{\boldsymbol{b}}(\tau) = -\hat{\boldsymbol{x}}_3.\end{aligned} \tag{C6}$$

In particular this implies that they are parallel and this condition is also maintained in the initial part of the dynamics as they rotate around the same axis. Therefore in this case

$$\tilde{\boldsymbol{b}}(t)\wedge\tilde{\boldsymbol{a}}(t) = 0 \quad\Longrightarrow\quad \tilde{\boldsymbol{G}}(t) = 0, \tag{C7}$$

making the entire trajectory a singular interval [hence satisfying (46)].

APPENDIX D: SINGULAR INTERVALS FOR THE HARMONIC OSCILLATOR DCP MODEL

Here we study the presence of singular intervals for the harmonic oscillator DCP model, i.e., time intervals during which the function $G_1(t)$ of Eq. (60) gets equal to zero. The fundamental observation is that in order to fulfill such constraint it is necessary to have not just $G_1(t) = 0$, but also $\frac{d^nG_1(t)}{dt^n} = 0\ \forall n$. Recalling Eq. (60) this implies

$$\begin{aligned}p_2(t) &= 2v_2(t)\,\omega_0,\\ \frac{d^np_2(t)}{dt^n} &= 2\frac{d^nv_2(t)}{dt^n}\,\omega_0.\end{aligned} \tag{D1}$$

By imposing the PMP conditions for optimality in (11), we have that the costates of the harmonic oscillator DCP model evolve in the following way:

$$\begin{aligned}\dot{p}_1(t) &= 0,\\ \dot{p}_2(t) &= -\omega_0[2\lambda_1(t)+p_3(t)] + 2p_1(t)\lambda_1(t),\\ \dot{p}_3(t) &= \omega_0 p_2(t),\end{aligned} \tag{D2}$$

with boundary condition $p_j(\tau) = 0$ for all j [notice that in particular this already tells us that $p_1(t) = 0$ for all t so that we can eliminate it from the list].

From Eq. (D1) with $n = 1$ and from Eqs. (56) and (D2) we have

$$\begin{aligned}\dot{p}_2(t) &= 2\omega_0\dot{v}_2(t) = -2\omega_0^2v_3(t) - 2\omega_0\lambda_1(t)\\ &= -\omega_0p_3(t) - 2\omega_0\lambda_1(t)\end{aligned} \tag{D3}$$

from which we get

$$p_3(t) = 2\omega_0v_3(t). \tag{D4}$$

In conclusion the conditions to be in a singular interval are

$$p_2(t) = 2\omega_0v_2(t), \quad p_3(t) = 2\omega_0v_3(t). \tag{D5}$$

Now since up to a constant rescaling $p_2(t)$ and $p_3(t)$ have the exact same evolution of $v_2(t)$ and $v_3(t)$, respectively, it is evident that if (D5) holds at a time t, then it will continue to be true until $t = \tau$. From the boundary conditions $\boldsymbol{p}(\tau) = 0$, we obtain that $v_2(\tau) = v_3(\tau) = 0$, i.e.,

$$\langle a\rho(\tau)\rangle = 0. \tag{D6}$$

Notice however that if we assume that the input state of the system is the ground state of H_0, then the above condition can only be verified if and only if $\rho(\tau)$ corresponds to the ground state itself (a condition that is certainly undesirable for an optimal control method that aims to increase the energy of the model). This fact follows from the observation that the Hamiltonian (55) can only induce displacements or phase shifts in the system, so that starting from the vacuum it will always produce coherent states. And the only coherent state that has zero expectation value for the annihilation operator is indeed the vacuum itself. This means that there cannot exist an optimal $\lambda_1^{\star}(t)$ that could enforce the condition for singularity.

APPENDIX E: HARMONIC OSCILLATOR FREQUENCY OPTIMIZATION

Here we show that, among all the bang-bang solutions that are optimal according to the results presented in Sec. V C, a square wave with a resonant frequency achieves the best performance in the long-time limit. From the dynamical equations for v_2 and v_3 in (57) we obtain

$$\ddot{v}_3(t) + \omega_0^2v_3(t) = -\omega_0\lambda_1(t). \tag{E1}$$

The differential equation above can be solved using the Green's-function approach. The retarded Green's function satisfying $[\frac{d^2}{dt^2}+\omega^2]G(t-t') = \delta(t-t')$ can be computed with the Fourier transform and reads

$$G(t-t') = \frac{1}{2\pi}\int_{-\infty}^{\infty}\frac{e^{-i\omega(t-t')}}{\omega^2+i\omega\epsilon-\omega_0^2}d\omega \tag{E2}$$

where $\epsilon > 0$ is a small parameter that we will send to zero at the end of the calculations. The general solution of (E1) is

$$v_3(t) = v_3(0)\cos(\omega_0 t) + \frac{\dot{v}_3(0)}{\sin(\omega_0 t)} - \int_0^t dt' \omega_0 G(t-t')\lambda_1(t'), \tag{E3}$$

which by initializing the battery in the ground state, i.e., by choosing $v_3(0) = \dot{v}_3(0) = 0$, reduces to

$$v_3(t) = \frac{1}{2\pi}\int_{-\infty}^{\infty} dt' \int_{-\infty}^{\infty} \frac{\omega_0 e^{-i\omega(t-t')}}{\omega^2 + i\omega\epsilon - \omega_0^2}\lambda_1(t')d\omega. \tag{E4}$$

Combining the results above with the first and the last of Eq. (56), we obtain that the charging power reads

$$v_1(t) = \frac{i}{\pi}\int_{-\infty}^{\infty} ds \int_{-\infty}^{\infty} dt' \int_{-\infty}^{\infty} \frac{\omega e^{-i\omega(s-t')}}{\omega^2 + i\omega\epsilon - \omega_0^2}\lambda_1(t')\lambda_1(s)d\omega, \tag{E5}$$

where the last integral is nonzero only in the interval $[0, \tau]$, that is, when the external driving force is switched on. After performing the integrals on the time variables we are left with

$$v_1(t) = \frac{i\omega_0}{\pi}\int_{-\infty}^{\infty} \frac{\omega|\lambda_1(\omega)|^2}{\omega^2 + i\omega\epsilon - \omega_0^2} d\omega. \tag{E6}$$

With the residue theorem, after sending ϵ to zero, the previous integral gives

$$v_1(t) \approx c[|\lambda_1(\omega_0)|^2 + |\lambda_1(-\omega_0)|^2], \tag{E7}$$

where c is a constant and the time dependence of v_1 is hidden in the parametric dependence of $\lambda_1(\omega)$ by time (remember that the control has to nullify outside $[0, t]$). From the equation above, we obtain that to maximize the total work in the long-time limit we have to choose a protocol that maximizes $|\lambda_1(\omega_0)|^2 + |\lambda_1(-\omega_0)|^2$. In the set of bang-bang protocols that we proved to be optimal, the best choice is a square wave with frequency ω_0.

[1] A. Acín, I. Bloch, H. Buhrman, T. Calarco, C. Eichler, J. Eisert, D. Esteve, N. Gisin, S. J. Glaser, F. Jelezko, S. Kuhr, M. Lewenstein, M. F. Riedel, P. O. Schmidt, R. Thew, A. Wallraff, I. Walmsley, and F. K. Wilhelm, The quantum technologies roadmap: A European community view, New J. Phys. **20**, 080201 (2018).

[2] M. F. Riedel, D. Binosi, R. Thew, and T. Calarco, The european quantum technologies flagship programme, Quantum Sci. Technol. **2**, 030501 (2017).

[3] R. Alicki and M. Fannes, Entanglement boost for extractable work from ensembles of quantum batteries, Phys. Rev. E **87**, 042123 (2013).

[4] G. M. Andolina, D. Farina, A. Mari, V. Pellegrini, V. Giovannetti, and M. Polini, Charger-mediated energy transfer in exactly solvable models for quantum batteries, Phys. Rev. B **98**, 205423 (2018).

[5] D. Farina, G. M. Andolina, A. Mari, M. Polini, and V. Giovannetti, Charger-mediated energy transfer for quantum batteries: An open-system approach, Phys. Rev. B **99**, 035421 (2019).

[6] G. M. Andolina, M. Keck, A. Mari, M. Campisi, V. Giovannetti, and M. Polini, Extractable Work, the Role of Correlations, and Asymptotic Freedom in Quantum Batteries, Phys. Rev. Lett. **122**, 047702 (2019).

[7] F. Binder, S. Vinjanampathy, K. Modi, and J. Goold, Quantacell: Powerful charging of quantum batteries, New J. Phys. **17**, 075015 (2015).

[8] F. Campaioli, F. A. Pollock, F. C. Binder, L. Céleri, J. Goold, S. Vinjanampathy, and K. Modi, Enhancing the Charging Power of Quantum Batteries, Phys. Rev. Lett. **118**, 150601 (2017).

[9] K. V. Hovhannisyan, M. Perarnau-Llobet, M. Huber, and A. Acín, Entanglement Generation is Not Necessary for Optimal Work Extraction, Phys. Rev. Lett. **111**, 240401 (2013).

[10] S. Montangero, T. Calarco, and R. Fazio, Robust Optimal Quantum Gates for Josephson Charge Qubits, Phys. Rev. Lett. **99**, 170501 (2007).

[11] S. Gherardini, F. Campaioli, F. Caruso, and F. C. Binder, Stabilizing open quantum batteries by sequential measurements, Phys. Rev. Res. **2**, 013095 (2020).

[12] D. Rosa, D. Rossini, G. M. Andolina, M. Polini, and M. Carrega, Ultra-stable charging of fast-scrambling syk quantum batteries, J. High Energy Phys. 11 (2020) 067.

[13] D. Ferraro, M. Campisi, G. M. Andolina, V. Pellegrini, and M. Polini, High-Power Collective Charging of a Solid-State Quantum Battery, Phys. Rev. Lett. **120**, 117702 (2018).

[14] J. Q. Quach, K. E. McGhee, L. Ganzer, D. M. Rouse, B. W. Lovett, E. M. Gauger, J. Keeling, G. Cerullo, D. G. Lidzey, and T. Virgili, Superabsorption in an organic microcavity: Toward a quantum battery, Sci. Adv. **8**, eabk3160 (2022).

[15] R. R. Rodriguez, B. Ahmadi, G. Suarez, P. Mazurek, S. Barzanjeh, and P. Horodecki, Optimal quantum control of charging quantum batteries, arXiv:2207.00094 (2022).

[16] F. Pirmoradian and K. Mølmer, Aging of a quantum battery, Phys. Rev. A **100**, 043833 (2019).

[17] F. Barra, Dissipative Charging of a Quantum Battery, Phys. Rev. Lett. **122**, 210601 (2019).

[18] J. Monsel, M. F. Asiani, B. Huard, and A. Auffèves, A coherent quantum engine based on bath and battery engineering, in *Rochester Conference on Coherence and Quantum Optics (CQO-11)*, paper W2A.2 (2019), doi: https://doi.org/10.1364/CQO.2019.W2A.2.

[19] D. Rossini, G. M. Andolina, and M. Polini, Many-body localized quantum batteries, Phys. Rev. B **100**, 115142 (2019).

[20] D. Rossini, G. M. Andolina, D. Rosa, M. Carrega, and M. Polini, Quantum Advantage in the Charging Process of Sachdev-Ye-Kitaev Batteries, Phys. Rev. Lett. **125**, 236402 (2020).

[21] M. T. Mitchison, J. Goold, and J. Prior, Charging a quantum battery with linear feedback control, Quantum **5**, 500 (2021).

[22] K. V. Hovhannisyan, F. Barra, and A. Imparato, Charging assisted by thermalization, Phys. Rev. Res. **2**, 033413 (2020).

[23] J.-Y. Gyhm, D. Šafránek, and D. Rosa, Quantum Charging Advantage Cannot Be Extensive without Global Operations, Phys. Rev. Lett. **128**, 140501 (2022).

[24] F. Barra, K. V. Hovhannisyan, and A. Imparato, Quantum batteries at the verge of a phase transition, New J. Phys. **24**, 015003 (2022).

[25] C.-K. Hu, J. Qiu, P. J. P. Souza, J. Yuan, Y. Zhou, L. Zhang, J. Chu, X. Pan, L. Hu, J. Li, Y. Xu, Y. Zhong, S. Liu, F. Yan, D. Tan, R. Bachelard, C. J. Villas-Boas, A. C. Santos, and D. Yu, Optimal charging of a superconducting quantum battery, Quantum Sci. Technol. **7**, 045018 (2022).

[26] D. Dong and I. Peteren, Quantum control theory and applications: A survey, IET Control Theory and Applications **4**, 2651 (2010).

[27] J. Werschnik and E. K. U. Gross, Quantum optimal control theory, J. Phys. B: At., Mol. Opt. Phys. **40**, R175 (2007).

[28] H. Mabuchi and N. Khaneja, Principles and applications of control in quantum systems, International Journal of Robust and Nonlinear Control **15**, 647 (2005).

[29] D. Stefanatos and E. Paspalakis, A shortcut tour of quantum control methods for modern quantum technologies, Europhys. Lett. **132**, 60001 (2020).

[30] U. Boscain, M. Sigalotti, and D. Sugny, Introduction to the pontryagin maximum principle for quantum optimal control, PRX Quantum **2**, 030203 (2021).

[31] H. M. Wiseman and G. J. Milburn, Quantum Theory of Optical Feedback via Homodyne Detection, Phys. Rev. Lett. **70**, 548 (1993).

[32] U. Boscain, G. Charlot, J.-P. Gauthier, S. Guérin, and H.-R. Jauslin, Optimal Control in laser-induced population transfer for two- or three-level quantum systems, J. Math. Phys. **43**, 2107 (2002).

[33] A. P. Peirce, M. A. Dahleh, and H. Rabitz, Optimal control of quantum-mechanical systems: Existence, numerical approximation, and applications, Phys. Rev. A **37**, 4950 (1988).

[34] A. Assion, T. Baumert, M. Bergt, T. Brixner, B. Kiefer, V. Seyfried, M. Strehle, and G. Gerber, Control of chemical reactions by feedback-optimized phase-shaped femtosecond laser pulses, Science **282**, 919 (1998).

[35] R. J. Levis, G. M. Menkir, and H. Rabitz, Selective bond dissociation and rearrangement with optimally tailored, strong-field laser pulses, Science **292**, 709 (2001).

[36] T. Caneva, M. Murphy, T. Calarco, R. Fazio, S. Montangero, V. Giovannetti, and G. E. Santoro, Optimal Control at the Quantum Speed Limit, Phys. Rev. Lett. **103**, 240501 (2009).

[37] V. Giovannetti, S. Lloyd, and L. Maccone, The speed limit of quantum unitary evolution, J. Opt. B: Quantum Semiclassical Opt. **6**, S807 (2004).

[38] S. Deffner and S. Campbell, Quantum speed limits: From Heisenberg's uncertainty principle to optimal quantum control, J. Phys. A: Math. Theor. **50**, 453001 (2017).

[39] G. C. Hegerfeldt, Driving at the Quantum Speed Limit: Optimal Control of a Two-Level System, Phys. Rev. Lett. **111**, 260501 (2013).

[40] C. P. Koch, Controlling open quantum systems: Tools, achievements, and limitations, J. Phys.: Condens. Matter **28**, 213001 (2016).

[41] R. Roloff, M. Wenin, and W. Ptz, Optimal control for open quantum systems: Qubits and quantum gates, J. Comput. Theor. Nanosci. **6**, 1837 (2009).

[42] L. S. Pontryagin, *Mathematical Theory of Optimal Processes* (CRC, Boca Raton, FL, 1987).

[43] D. E. Kirk, *Optimal Control Theory: An Introduction* (Courier, New York, 2004).

[44] V. Cavina, A. Mari, A. Carlini, and V. Giovannetti, Variational approach to the optimal control of coherently driven, open quantum system dynamics, Phys. Rev. A **98**, 052125 (2018).

[45] V. Cavina, A. Mari, A. Carlini, and V. Giovannetti, Optimal thermodynamic control in open quantum systems, Phys. Rev. A **98**, 012139 (2018).

[46] D. Stefanatos, Maximising optomechanical entanglement with optimal control, Quantum Sci. Technol. **2**, 014003 (2017).

[47] C. Lin, D. Sels, and Y. Wang, Time-optimal control of a dissipative qubit, Phys. Rev. A **101**, 022320 (2020).

[48] D. Stefanatos and E. Paspalakis, Speeding up adiabatic passage with an optimal modified Roland-Cerf protocol, J. Phys. A: Math. Theor. **53**, 115304 (2020).

[49] W. Niedenzu, M. Huber, and E. Boukobza, Concepts of work in autonomous quantum heat engines, Quantum **3**, 195 (2019).

[50] R. Salvia and V. Giovannetti, On the distribution of the mean energy in the unitary orbit of quantum states, Quantum **5**, 514 (2021).

[51] M. Lapert, Y. Zhang, M. Braun, S. J. Glaser, and D. Sugny, Singular Extremals for the Time-Optimal Control of Dissipative Spin 1/2 Particles, Phys. Rev. Lett. **104**, 083001 (2010).

[52] D. Stefanatos and E. Paspalakis, Optimal shortcuts of stimulated Raman adiabatic passage in the presence of dissipation, Phil. Trans. R. Soc. A **380**, 20210283 (2022).

[53] H. E. D. Scovil and E. O. Schulz-DuBois, Three-Level Masers as Heat Engines, Phys. Rev. Lett. **2**, 262 (1959).

[54] R. Alicki, The quantum open system as a model of the heat engine, J. Phys. A: Math. Gen. **12**, L103 (1979).

[55] R. Kosloff, A quantum mechanical open system as a model of a heat engine, J. Chem. Phys. **80**, 1625 (1984).

[56] W. Pusz and S. L. Woronowicz, Passive states and KMS states for general quantum systems, Commun. Math. Phys. **58**, 273 (1978).

[57] A. Lenard, Thermodynamical proof of the Gibbs formula for elementary quantum systems, J. Stat. Phys. **19**, 575 (1978).

[58] P. Skrzypczyk, R. Silva, and N. Brunner, Passivity, complete passivity, and virtual temperatures, Phys. Rev. E **91**, 052133 (2015).

[59] R. Salvia and V. Giovannetti, Energy upper bound for structurally stable n-passive states, Quantum **4**, 274 (2020).

[60] M. Esposito and C. V. den Broeck, Second law and Landauer principle far from equilibrium, Europhys. Lett. **95**, 40004 (2011).